Author's Response

Dear reviewers and editors,

as suggested we carefully checked the manuscript and technical report and found a few typographical errors, which we corrected. Additionally we added the source of the DEM depicted in Figure 3.

Kind Regards

Thomas Bueche

glmGUI v1.0: an R-based Geographical User Interface and toolbox for GLM (General Lake Model) simulations

Thomas Bueche [12], Marko Wenk [3], Benjamin Poschlod [1], Filippo Giadrossich [4], Mario Pirastru [4], Mark Vetter [5]

[1]Department of Geography, Ludwig-Maximilians-University Munich, Germany
[2]WipflerPLAN Planungsgesellschaft mbH, Pfaffenhofen a. d. Ilm, Germany
[3]Independent Scholar, Stuttgart, Germany
[4]Dipartimento di Agraria, Unversity of Sassary, Italy
[5]Faculty of Plastics Engineering and Surveying, University of Applied Sciences Würzburg-Schweinfurt, Germany

10   *Correspondence to*: Thomas Bueche (tbueche@web.de)

Abstract. Numerical modeling provides the opportunity to quantify the reaction of lakes on alterations in their environment, such as changes in climate or hydrological conditions. The one-dimensional hydrodynamic General Lake Model (GLM) is an open-source software and widely used within the limnological research community. Nevertheless, neither an interface to process the input data and run the model, nor tools for an automatic parameter calibration yet

15   exist. Hence, we developed *glmGUI*, a Geographical User Interface (GUI) including a toolbox for an autocalibration, parameter sensitivity analysis, and several plot options. The tool is provided as a package for the freely available scientific code language R. The model parameters can be analyzed and calibrated for the simulation output variables water temperature and lake level.

The *glmGUI* package is tested for two sites (Lake Ammersee, Germany, and Lake Baratz, Italy) distinguishing in size,

20   mixing regime, hydrology of the catchment area (i.e. the number of inflows and their runoff seasonality), and climatic conditions. A robust simulation of water temperature for both lakes (Ammersee: RMSE = 1.17 °C, Baratz: RMSE =1.30°C) is achieved by a quick automatic calibration. The quality of a water temperature simulation can be assessed immediately by means of a difference plot provided by *glmGUI*, which displays the distribution of the spatial (vertical) and temporal deviations. The calibration of the lake level simulations of Lake Ammersee for multiple hydrological

25   inputs including also unknown inflows yielded a satisfactory model fit (RMSE = 0.20 m). This shows that GLM can also be used to estimate the water balance of lakes correctly. The tools provided by *glmGUI* enable a less time-consuming and simplified parameter optimization within the calibration process. Due to this, the free availability and the implementation in a GUI, the presented R package expands the application of GLM to a broader field of lake modeling research and even beyond limnological experts.

1 Introduction

As lakes respond to changes in their environment they are often considered to be "sentinels of change" (Williamson et al., 2009, ~~Hipsey et al., 2017~~, Hipsey et al., 2019). The investigation of alterations in the physical conditions of lakes, such as water temperature, stratification, water balance, mixing behavior, or ice cover, has a key role in the understanding of the lake dynamics. Numerical modeling provides the opportunity of research beyond the analysis of

35   observational monitoring data (Frassl et al., 2016), enabling simulations of periods without in-situ data as well as future conditions of lakes.

The development and application of community-based models is of increasing importance in order to find solutions for the future challenges to simulate water body conditions under environmental alterations (e.g. climatic, land use, and

agricultural policies, Bruce et al., 2018).The one-dimensional hydrodynamic General Lake Model (GLM) has been developed, under the leadership of members of the Global Lake Ecological Observatory Network (GLEON, gleon.org, Hanson et al., 2016), in response to the need of a robust model of lake dynamics (~~Hipsey et al., 2017~~Hipsey et al., 2019), which is applicable for the vast diversity of lakes and reservoirs around the globe. GLM is able to simulate the

5 thermal dynamics of lakes in their temporal and spatial (vertical) characteristics. The model code is open-source and applied in numerous studies to a broad variety of different lakes and research questions (e.g., Bueche et al., 2017; Bucak et al., 2018; Bruce et al., 2018; Fenocchi et al., 2018; Robertson et al., 2018; Ladwig et al., 2018; Mi et al., 2018; Fenocchi et al., 2017; Fenocchi et al., 2019). Carey and Gougis (2017) present the usage of GLM beyond the research application incorporated in a teaching tool for students.

10 Despite the high applicability of GLM a powerful toolbox for automatic calibration, validation and statistical sensitivity analysis is not yet existent. Therefore, we developed an R-based Geographical User Interface (GUI) implemented in the new R package *glmGUI* combining an easy handling of GLM simulations, a tool to automatize the calibration process, and visualization options for the input and output data. In general, the maxim of our project was inspired by four aspects:

15 • Provision of an open-source tool

- Provision of a user-friendly tool, which could be used by experts as well as less experienced modelers and limnologists
- Using scripts to adapt the tool, with high acceptance and contribution in the scientific community
- Flexibility for the implementation of different calibration parameters and for the numerical and graphical

20 interpretation of the output results

The R language (https://www.r-project.org) was chosen because it is open-source, flexible and an independent platform (Snortheim et al., 2017). Moreover, the lake modeler community uses already R based packages, i.e. *glmtools* for parameterization or plotting model output (https://github.com/USGS-R/glmtools) and *rLakeAnalyzer* for post-processing and evaluation of the model results (Winslow et al., 2016, https://github.com/GLEON/rLakeAnalyzer).

25 Changes in the water level of a lake can have strong influences on hydrodynamics, such as thermocline depth and stratification stability and duration, and can also affect lake water quality (Robertson et al., 2018). The appropriate water level reproduction by lake models is essential for a robust simulation of spatial features of thermal dynamics in lakes, especially in shallow lakes with high variations in water stages. Furthermore, an accurate simulation of the lake level ensures the correct representation of hydrological interaction of the lake with its environment in the catchment

30 area. Hence, in addition to the model output water temperature, the lake level is included to be calibrated in the provided automated calibration tool.

In this contribution we present the options included in *glmGUI* and show the application for two different sites, namely the pre-alpine deep Lake Ammersee, south Germany, and the shallow, Mediterranean Lake Baratz, Sardinia, Italy. The objectives of these two case studies are the calibration of the water temperature and lake level simulations of GLM

35 using the automatic calibration tool.

2 Lake model, software description, and toolbox options

2.1 The hydrodynamic lake model

The GLM is a one-dimensional hydrodynamic model simulating the vertical profiles of temperature, salinity, and density at one spatial point in a lake over time (Frassl et al., 2016; Robertson et al., 2018). It applies the Lagrangian

40 layer structure adapting the thickness and volume of layers with uniform properties from each simulation step (Bueche

et al., 2017). The underlying equations and hydrodynamics closures are documented in Hipsey et al. (2014) and Hipsey et al. (2017). The hydrodynamic model can also easily be coupled with the Aquatic Ecodynamics library (AED2) to simulate water quality simulations (Weber et al., 2017; Bruce et al., 2018).

GLM simulations are based on parameterizations of mixing processes, surface dynamics, and the effect of inflows and outflows. The model performance of simulating the lake thermal dynamics as well as the water balance can be improved by a calibration of lake-specific parameters. The model documentation of Hipsey et al. (2017) includes also a description of the lake specific parameters and the default values for GLM simulations. The model requires meteorological and hydrological input data (see Table A1). Field data of water temperature should be available in a suitable temporal and spatial (several depths) resolution to enable a reliable calibration process.

2.2 R package *glmGUI*

The R package *glmGUI* is a self-written extension in R interacting with the functionality of GLM. It provides two basic application functions - the logical elements of model-fit criteria calculations and graphical user interfaces for data visualization. The package requires a software version of R of $\geq$ 3.4 and the version of *rLakeAnalyzer* $\geq$ 1.8.3. All required R packages are automatically installed during the first installation of *glmGUI*.

2.3 Graphical User Interface

The Graphical User Interface is constructed as a window based design using functions of the R package *gWidgets* (Verzani, 2014), which provides several toolkits for producing user interfaces by creating e.g. labels, buttons, containers, or drop lists. The GUI is organized in a main menu with five sections. Submenus and result messages are opened in separate windows (Fig. 1).
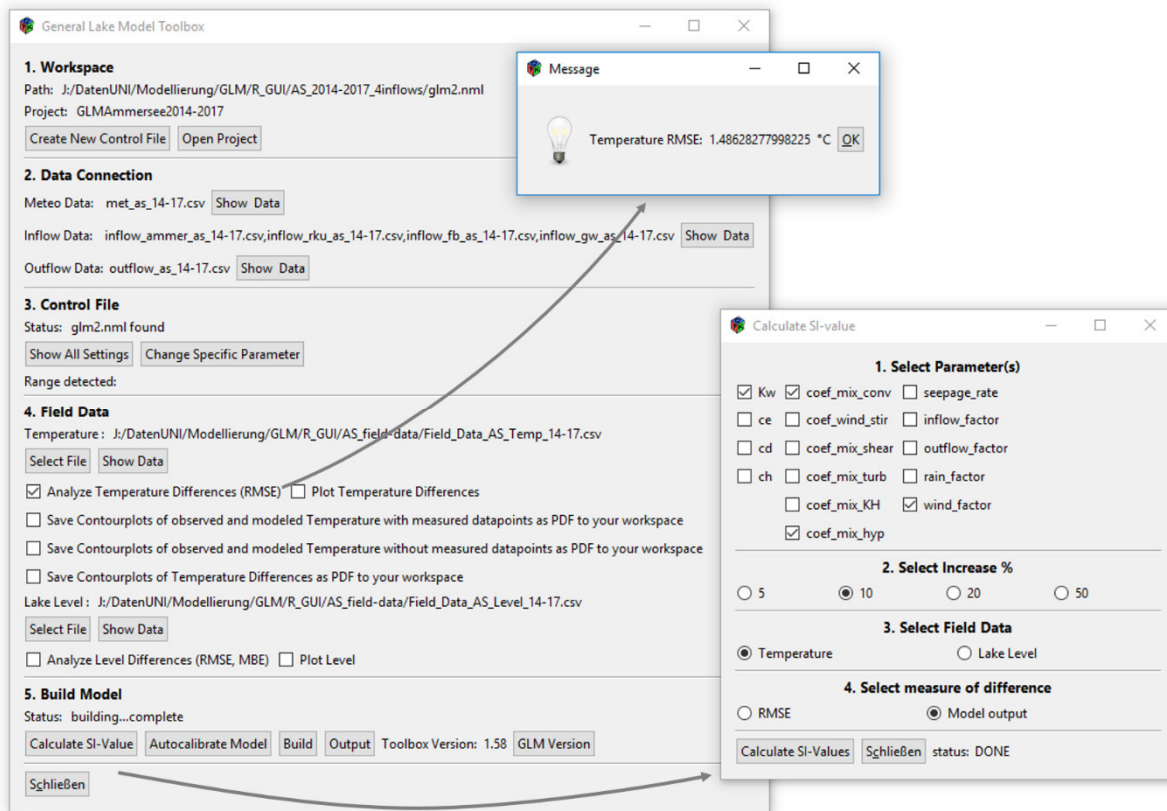

Fig. 1: Window-based structure of glmGUI with examples of the submenu 'Calculate SI-value' and of the result message 'Temperature RMSE' created after a model run.

3

2.3.1 Data pre-processing and model efficiency

The GUI enables either the usage of an existing simulation control file of GLM (glm2.nml) from a selectable workspace (section 1, Fig. 1), or the creation of a new control file using the function nml_template_path() of the R package *GLMr* (https://github.com/GLEON/GLMr). The lake specific parameters and settings are in accordance with the deposited file of *GLMr* and is due to change with the current GLM version. The input data are automatically listed in section 2 (Fig. 1), if stored at the path as specified in the control file. All included time series of input data can be visualized and tested against missing values (NA). The toolbox includes an option to fill the missing values applying the non-parametric Kalman-filter method (Grewal, 2011) using the R package *imputeTS* (Hyndman and Khandakar, 2007). Several filter methods were tested by manually removing values from existing time series of meteorological data and interpolating these missing values. The Kalman smoothing could deliver the best and most constant results for all kinds of the various meteorological data. If selected, an autofill option writes the interpolated values directly to the input file. All parameter settings defined within the control file can be shown and changed by the GUI (section 3, Fig. 1).

The model simulation can be run (section 5, Fig. 1) and several plot options can be selected to compare the model result with observed field data (section 4, Fig. 1). As lake level variations can have a strong impact on the water temperature distribution within lakes (especially true for shallow waters), the validation of the lake level simulation results is provided within the GUI additionally to the water temperature. The root mean square error (RMSE), which is often applied as model fit criteria in lake modeling studies (e.g. Bueche et al., 2017; Luo et al., 2018; Frassl et al., 2018), can be computed for both model output variables. Additionally, the mean bias error (MBE, average of the lake level differences of all time simulated time steps) is calculated for lake level simulations. Both model criteria are calculated for all available observed data points and averaged subsequently.

2.3.2 Plots and output visualization

Plot options are provided by *glmGUI* for the input time series in section 2 (Fig. 1) and for all output variables generated by GLM (csv and netCDF, section 5). This includes simple line plots (e.g. for lake level or evaporation) and contour plots for parameter varying in lake depth, such as water temperature or density. In addition, two types of contour plots of the vertical profile can be created. First is the visualization of observed and modeled water temperatures in one plot above each other with the option of the measured data as point-overlay to mark where and when field data are available (areas in between are interpolated to draw the plots, Fig. 2). Second plot visualizes the temperature differences between the interpolated measured values and the modeled data. This plot type is a new feature enabling a quick overview on the spatial and temporal errors and deviations of the simulation (Fig. 9). The displayed deviations are fixed to 9 classes in the range of the errors between -5 °C to +5 °C and all values beyond these limits are shown in one color (≤ -5 in dark blue and ≥ 5 in red) summarizing and highlighting extreme errors. The spatial reference in both plots is the lake surface, but lake level variations are represented by changes in depth, which become visible at the "bottom" of this plot type.

The generation of the contour plots is based on functions provided by *glmtools*. The default settings to scale the color bar legend for water temperature plots take into account the range of temperatures and also erroneously the range of lake depth. This method is adopted in glmGUI, while discarding the consideration of the lake depth, and the temperature range is adjusted explicitly to the plotting method to provide well differentiated color ranges in the legend.
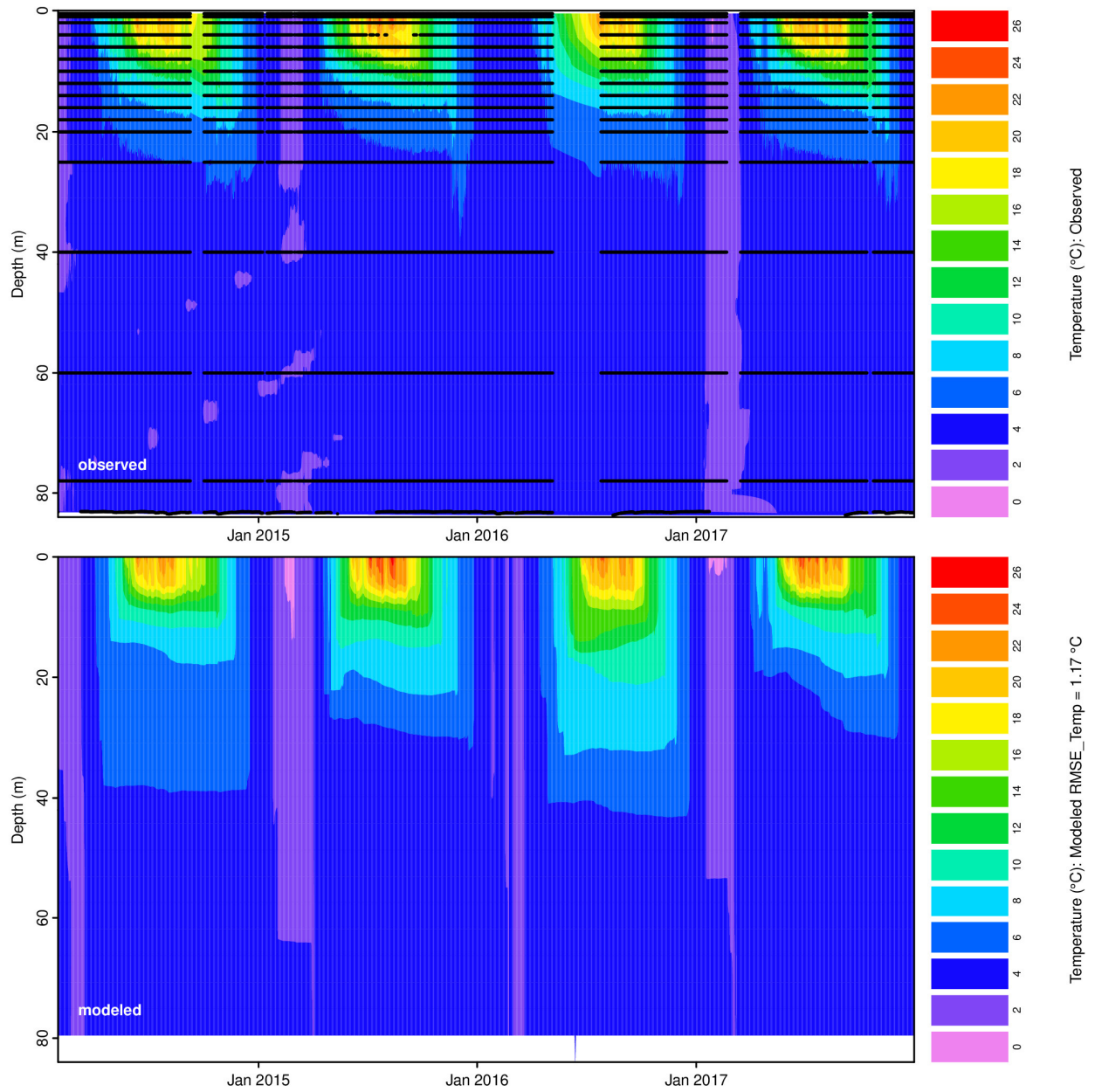
Fig. 2: Example of a contour plot of observed (top) and modelled (below) water temperatures for Lake Ammersee. Black dots mark the availability (time/date and depth) of observed water temperatures.

2.3.4 Sensitivity analysis

5   To reduce the effort of the model calibration process only sensitive parameters should be included (Luo et al., 2018), which usually are identified applying a sensitivity analysis. It investigates how variations in the output of a numerical model can be attributed to variations of input parameters or factors (Pianosi et al., 2016). The widely used approach after Lenhart et al. (2002) is implemented in the GUI. The Sensitivity Index (SI) is calculated for each selected parameter separately, since only one parameter is changed at a time:

10

$$SI = \frac{(y_1 - y_2)/y_0}{2\Delta x/x_0} \qquad (1)$$

5

The parameter with the value x_0 is increased and decreased by Δx. The resulting outputs y_1 and y_2 (either water temperature, lake level or the respective RMSEs) are subtracted and normalized by the output y_0, which results from using the unchanged parameter value x_0. Δx can be set to four different values in the GUI (5%, 10%, 20%, 50%). It can be chosen out of four grades of relative changes of a parameter. The sensitivity of the simulation can be analyzed concerning the model output of water temperature or lake level. SI-values can be calculated based on either the respective model output or the RMSE, as also applied by Rigosi et al. (2011).

2.3.4 Autocalibration

Since the GLM uses empirical equations (Hipsey et al., 2017), model parameters can be adjusted during the calibration process to minimize the error between model output and observations (Luo et al., 2018). As an alternative to adjust the parameters manually in the glm2.nml-file, *glmGUI* provides an automatic calibration tool for preselected parameters of surface dynamics, mixing parameters, and hydrological and meteorological factors (Table A2~~1~~). The user can choose out of those parameters that are to be included in the calibration process and define a percentage range, by which the upper and lower limit of every parameter is changed from the value in the glm2.nml-file. The resolution of the increase/decrease of the parameters within the defined limits can be set as well. According to these settings, model runs of GLM are executed with all possible combinations of the selected parameters ("brute-force"). The overall RMSE of the lake level or water temperature is calculated and saved for every parameter combination to a csv file, with the "best fit" being indicated.

The automated calibration of the lake level includes also the optimization for the parameter *inflow_factor* for multiple lake inflows. This enables an approximation to the water balance and the reproduction of the lake level, if the contribution of inflows is unknown, which is often the case for groundwater inflows or smaller tributaries.

The runtime of the calibration algorithm (t_{cal}~~t_cal~~) increases exponentially with the number of parameters (*p*) to be calibrated (Eq.(**2**))

$$t_{cal} = r^p * (t_{GLM} + t_{RMSE}) \tag{2}$$

with *r* as the number of tested values for each parameter p and t_{GLM}~~t_GLM~~, t_{RMSE}~~t_RMSE~~ as runtimes of the lake model and the calculation of the output RMSE.

3 Case study Lake Baratz

3.1 Study site

Lake Baratz is located in the northwest of Sardinia (Fig. 3), Italy, and is the only natural lake of the island. The elevation of its bottom is 18.6 m a.s.l. and the lake level suffered significant changes in the last two decades with a maximum lake depth of 11 m and a minimum of 3 m (Giadrossich et al., 2015; Niedda et al., 2014). The overflow spillway of the lake is at 32.5 m a.s.l. (Niedda et al., 2014). At this maximum level the lake has a surface of about 0.6 km² and volume of 5.1×10^6 m³ (Giadrossich et al., 2015). As lake-overflow events to the sea were extremely rare in the past century the catchment area can be considered as a closed-basin (Niedda and Pirastru, 2013). The lake watershed is about 12 km² with a maximum elevation of 410 m (Pirastru and Niedda, 2013). The only significant tributary is inflowing the lake in the northeast and drains a sub-catchment area of 8.1 km². Due to a very dry summer season the water inflow starts usually in December and ends in May (Giadrossich et al., 2015).

The lake can be classified as eutrophic and the water is brackish. Thermal stratification usually establishes in February or early March and lasts to early autumn (Giadrossich et al., 2015). Lake mixing occurs all throughout winter and thus, it can be classified as a warm monomictic lake.
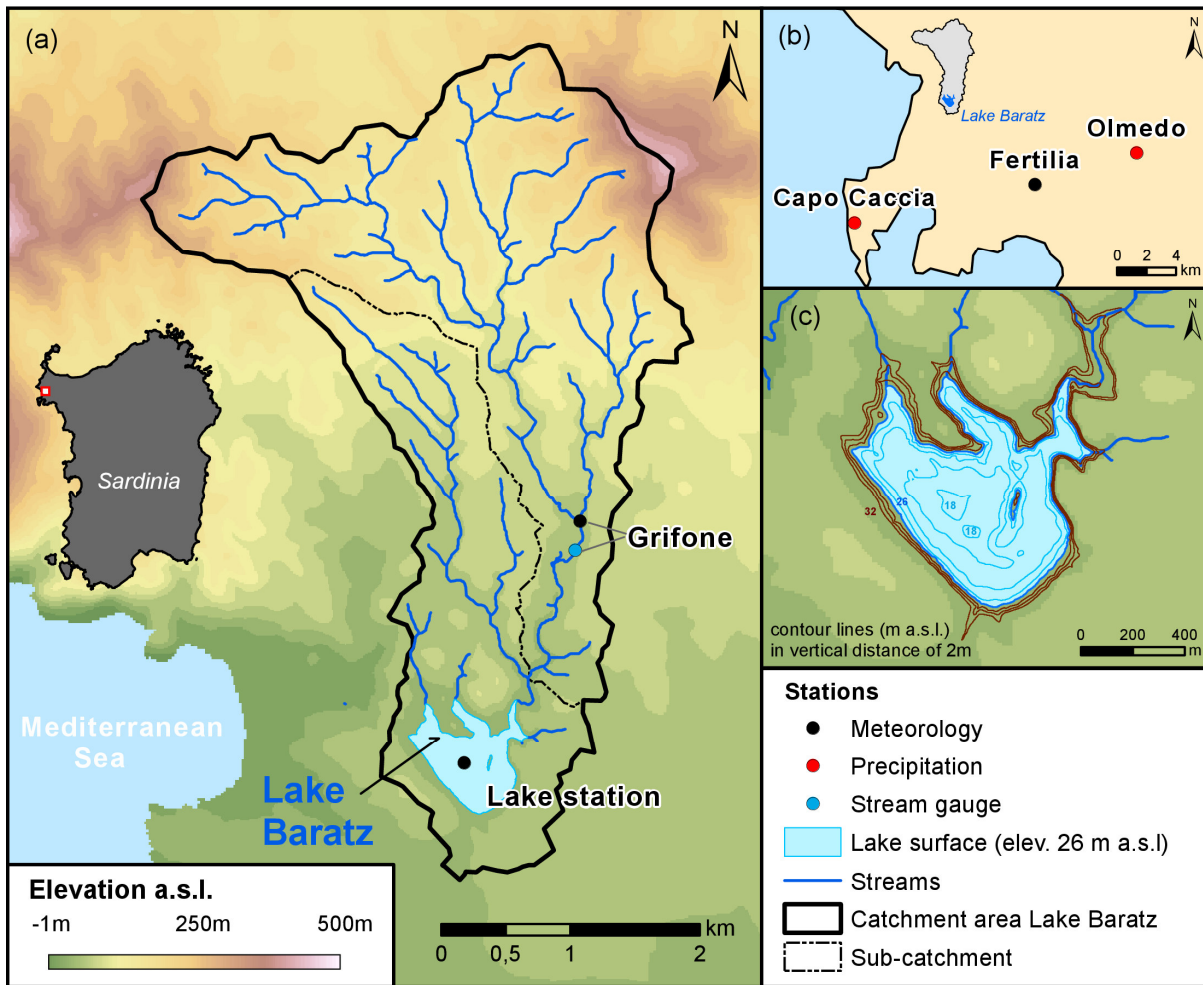
Fig. 3: a) Lake Baratz and its hydrological catchment area and observation station, b) Observation stations outside of the lake watershed (grey area), c) Contour lines of the lake basin. The blue area indicates the lake surface at a lake level of 8 m (equal to an elevation of 26 m a.s.l) observed in November 2012. Brown lines display dry terrain and cyan isobaths at this lake level (Source DEM © Regione Autonoma della Sardegna).

3.2 Sensitivity analysis and calibration

The simulation period for Lake Baratz is determined to be 13.07.2011 to 31.12.2016. We assume the light extinction coefficient value $K_w = 0.57$ m^{-1} is representative of the whole study period. K_ww is calculated dividing the Secchi-disk constant (in this case the minimum value of 1.44 was taken as it usually ranges between 1.44 and 1.80, Hornung, 2002; Holmes, 1970; Chapra, 2008) by the mean Secchi-disk depth of 2.50 meters (data from June 2016 to June 2017). A similar value can be obtained considering a Secchi-disk average depth of 3 meters (assumed when the lake had a higher water level) and Secchi-disk constant of 1.70 (Poole and Atkins, 1929). A further detailed description on the applied meteorological and hydrological model input data, the field data, and the data processing can be found in the Supplementary1 Material.

The calibration process of the lake level was accomplished without hydrological parameters, as preliminary estimations of the water balance considering the seasonality of the inflow and subsurface outflow already exist (see Supplementary Material S1.3Appendix A3.3), which are also applied in this study. Thus, the sensitivity analysis was performed considering only the parameters of surface dynamics and the *wind_factor* as wind can have an impact on the lake level due to its influence on evaporation. The options of 10 % increase and the RMSE as measure of deviation were selected.

7

After Lenhart et al. (2002) only one of four parameters (*cd*) is found to have a negligible sensitivity indicated by a SI-value of below 0.01. The analysis revels a high sensitivity for the parameters *ch* (SI = 0.234, see also Fig. 4) and *ce* (SI = 0.334) and a medium for *wind_factor* (SI = 0.089).

The sensitivity analysis regarding water temperature was conducted for parameters of lake mixing, surface dynamics, and the wind factor with the same options as selected for the lake level. Negligible SI-values of 0.005 and below are found for all considered parameters except for *ce* (SI = 0.232) and *wind_factor* (0.290) with a high sensitivity, and *ch* (0.050) with a sensitivity at the threshold between medium and small (Fig. 4). According to both sensitivity analyses the model is calibrated first for the lake level considering these three parameters with medium and high sensitivity. As the model is found to be sensitive in lake level and water temperature simulations for changes in the same parameters, the calibration for water temperature simulations was performed only considering *ce* and *wind_factor* to prevent a decline of the lake level reproduction by the water temperature calibration. Not considering parameter *ch*~~ch~~ is plausible, as its SI value matches only just the threshold to be medium sensitive. In addition, small parameter value ranges of 10 % are applied. Within the calibration process a total number of approx. 3000 simulation runs were conducted in six~~6~~ autocalibration runs.
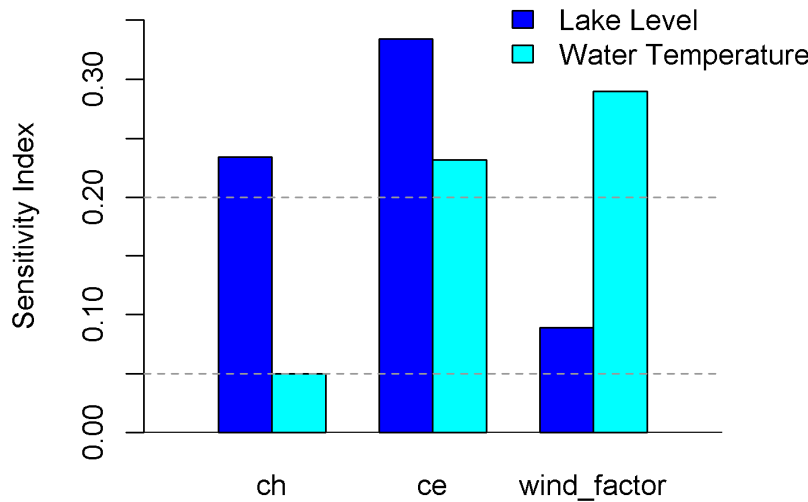

Fig. 4: Sensitivity Index (SI) after Lenhart et al. (2002) of GLM simulations of Lake Baratz regarding the lake level (blue) and water temperature (cyan). The lower horizontal line (SI = 0.05) marks the threshold between small and medium sensitivity, the upper line (SI = 0.20) between medium and high sensitivity.

3.3 Simulation results The calibration processes for lake level simulations of the lake model reveals the best fit when applying an unchanged parameter value for *ch* and an adjustment of *ce* to 0.001748 and of *wind_factor* to 1.56. The simulated lake level of Lake Baratz shows very good model fit criteria of an average RMSE = 0.11 m and an average MBE = 0.05 m. The seasonal pattern of the lake level, characterized by a strong increase during winter and a drop during summer, is represented well. Additionally, the general decrease of the water stage by about 3 m during the simulation period is simulated correctly, which proves the capability of the model to reproduce the water balance of the lake and its catchment area.
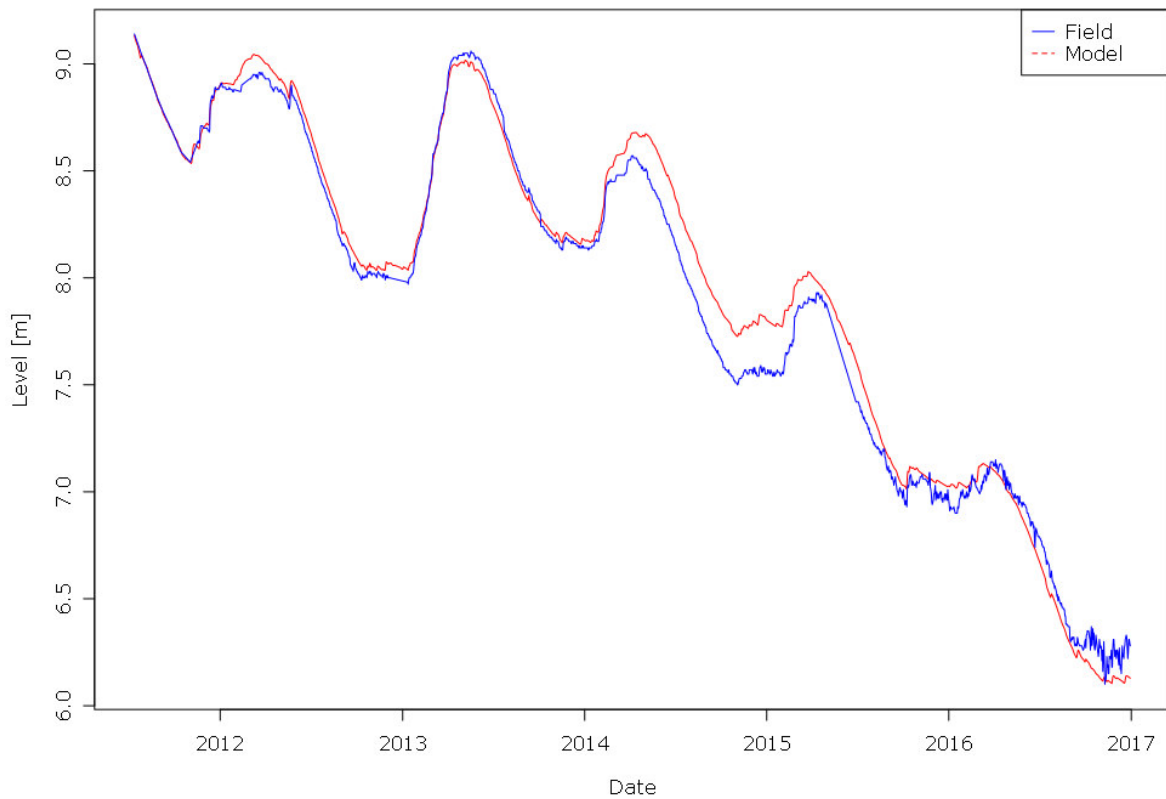
Fig. 5: Observed (blue) and simulated (red) lake level of Lake Baratz.

The modeled water temperatures simulated with the adapted lake parameters found by the (auto-)calibration yield an overall average RMSE of 1.30 °C. A period of remarkable deviation of simulated and observed lake level is induced in

5   January 2014, which could be attributed to uncertainties in the discharge input data simulated by a hydrological model. The basin in that period of the year is still in an intermediate status of soil moisture. Probably the hydrological model overestimated the discharge on the base of rainfall events in January 2014 which in reality did not produce a significant lake level variation (see Fig. 2 in Giadrossich et al., 2015). However, the observed and simulated lake levels in Fig. 5 have the same trend and the error caused in January is propagated throughout the year.

10 The model reproduces stratified and isothermal conditions (Fig. 6). A detailed overview on the temporal and spatial differences between the observed and simulated water temperatures is given in Fig. B1. The simulation can be assessed as a robust fit (Bruce et al., 2018), especially when considering the high degree of thermal dynamics due to the shallow depth of the lake and an additional enhancement by highly variable lake level (Fig. 6). The results approve also GLM to be applicable for shallow lakes in warm climates with high variety in lake level.
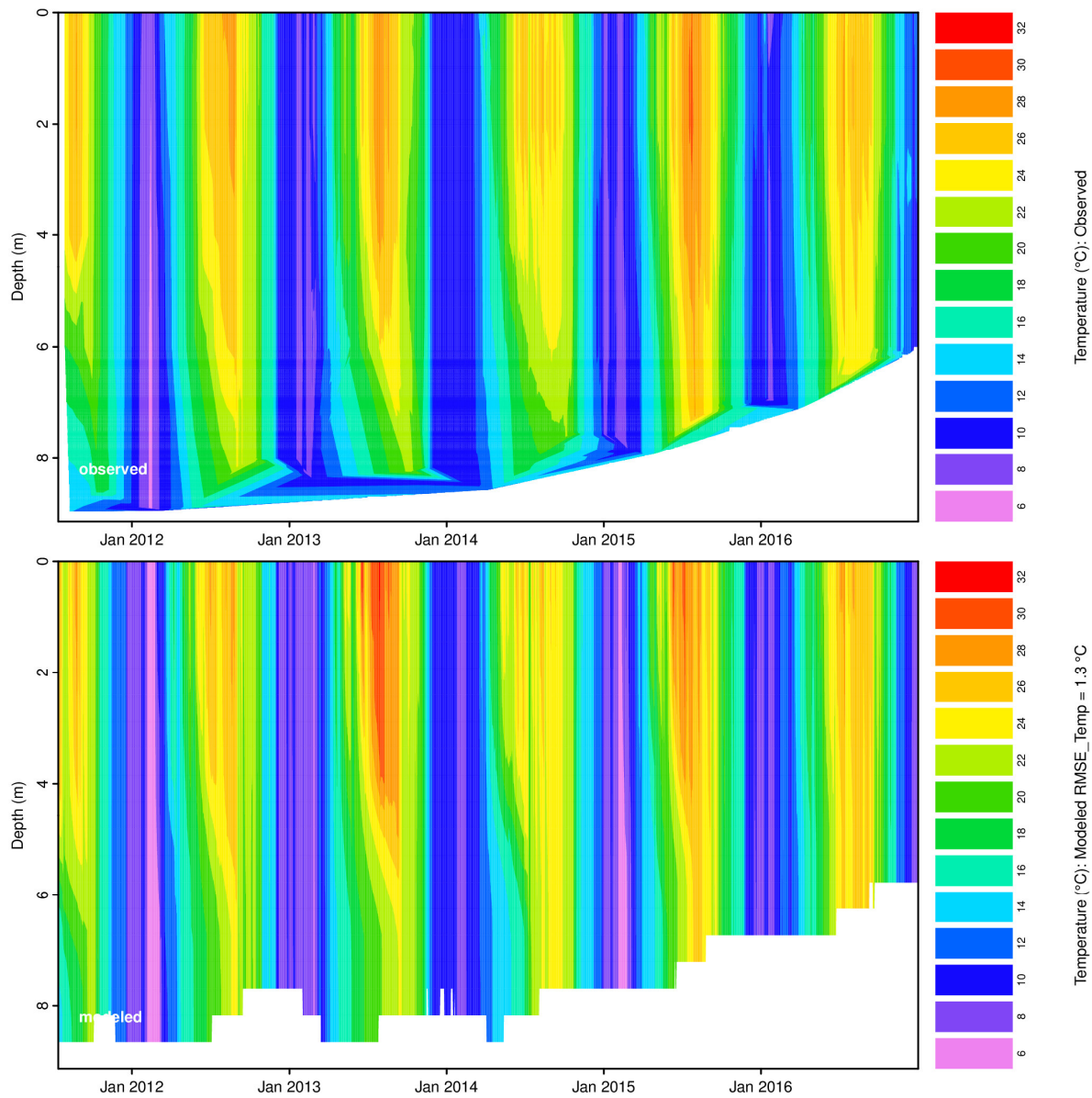
9

Fig. 6: Observed (top) and simulated (bottom) water temperatures of Lake Baratz.

4 Case study Lake Ammersee

4.1 Study site

The pre-alpine Lake Ammersee (Fig. 7) has a maximum depth of 83.7 m (Fig. S8, Supplementary Material), a surface area of 46.6 km² and a volume of about 1.8×10^9 km³ (Bueche and Vetter, 2014b). The mixing regime can be classified as dimictic, but also monomictic seasons occur (Bueche, 2016). The trophic status is currently mesotrophic (Vetter and Sousa, 2012).

The lake has a catchment area of about 994 km² and its outflow in the north (Stegen gauge station). The main tributary is River Ammer, which contributes approximately 80 % of the total annual discharge to the lake (Bueche and Vetter, 2015). Several other streams and creeks inflow into the lake, but only River Rott and Fischbach have a share of greater than 5 % of the total lake catchment area size (see~~Fehler! Verweisquelle konnte nicht geunden werden.7~~ **Fig. 7** ~~Suppl. Material~~). Additionally, groundwater is assumed to inflow the lake, which has not been quantified yet (Bueche and Vetter, 2014a). The mean lake level is 532.9 m a.s.l. and usually varies about 1 m (Bay. LfU, 2018).
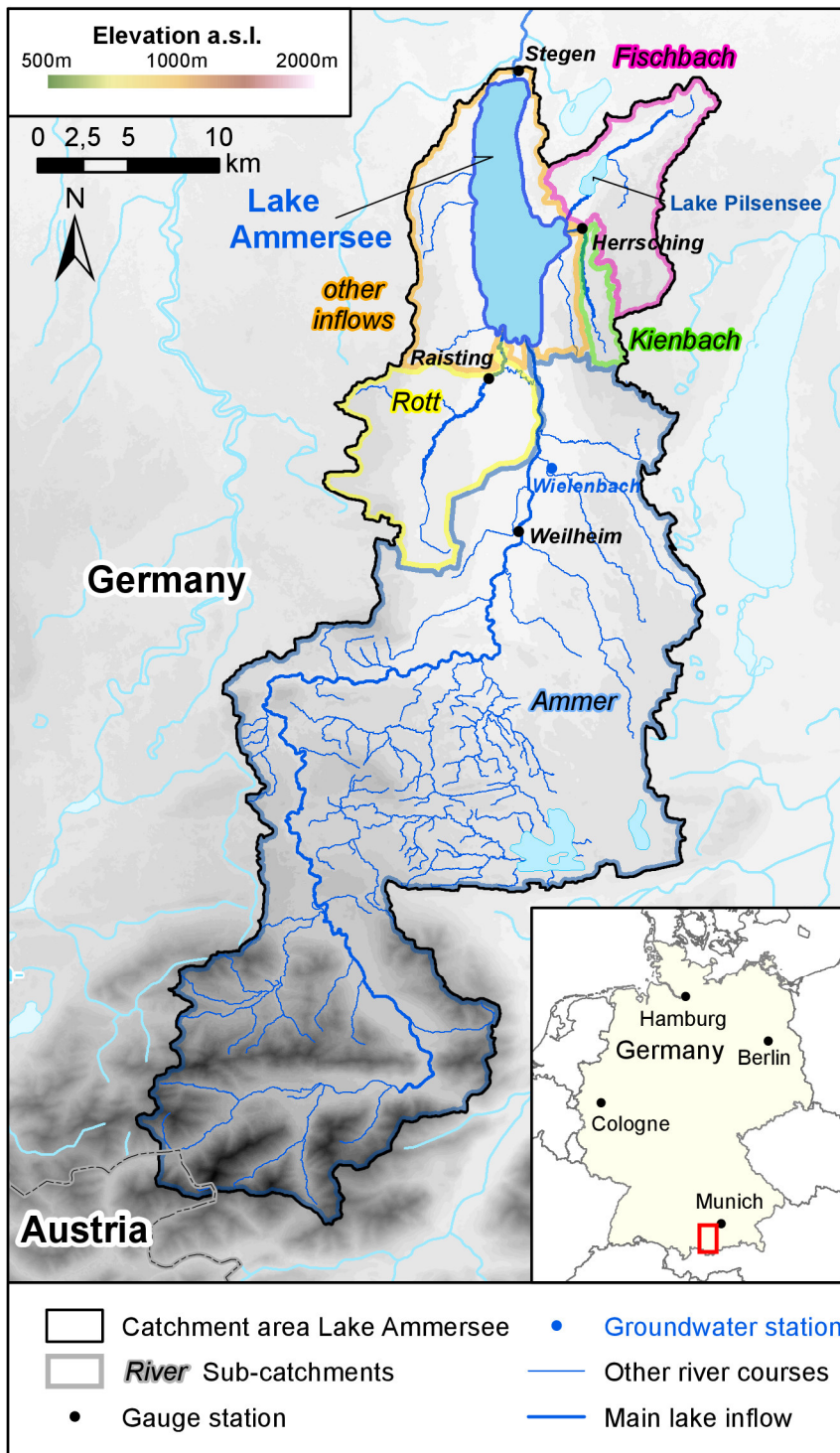
15

10

Fig. 7: Catchment area (with sub-catchments) of Lake Ammersee. Dots mark the locations of hydrological observation stations (Source DEM: Elevation data from ASTER GDEM, a product of METI and NASA, Source geo-data: Geobasisdaten © Bayerische Vermessungsverwaltung, www.geodaten.bayern.de).

4.2 Sensitivity analysis and calibration

The simulation period for Lake Ammersee is chosen to be 30.01.2014 to 31.12.2017 starting when reliable field data of the lake station is available consistently (see Supplemental Material, section 2). The initial profile of water temperatures is taken from the observations of that date. No water quality data were available for the simulation period and the salinity values are derived from conductivity measurements of January 2004, when similar thermal conditions of a slight inverse stratification were prevailed and equivalent salinity conditions can be assumed. As the trophic status has not changed since 2004 the average value K_W of 0.35 m^{-1} determined for the period 2004 to 2008 from secchi-disk

observations (data surveyed and provided by Bavarian Environment Agency) is used for the GLM simulations in this study.

The calibration of the lake level considers the *inflow_factor*~~inflow_factor~~ (i.e. simple factor for the discharge values of the inflows) of the four defined inflows of River Ammer, River Fischbach, groundwater inflow, and the sum of River

5 Rott, River Kienbach, and all other unknown inflows. Thus, the adjustment of the representative *inflow_factor* includes the required correction of the available discharge data considering the observations are not taken at the stream inlet to the lake but at an upstream location. This is especially relevant for River Ammer with its gauge at Weilheim (Fig. 7). Meteorological input data are taken by a raft station at the lake center except for precipitation and cloud cover data (see ~~Supplemental~~ Supplementary Material, section 2, for a detailed description about the sources of the used meteorological

10 and hydrological input data and the processing of the data).

The sensitivity analysis regarding the water temperature (increase: 10 %, measure of difference: RMSE) reveals seven parameters with an SI > 0.05 indicating a medium sensitivity (after Lenhart et al., 2002, Table 1). In order to reduce the calculation time of the autocalibration runs, four parameters of high sensitivity with a SI above 0.2 are chosen for this process. In total approx. 50000 simulation runs in 12 autocalibration runs were performed within the calibration

15 process.

Table 1: Values of SI for Lake Ammersee water temperature simulations.

Parameter	SI
ch	0.534
coef_mix_shear	0.484
coef_mix_turb	0.410
wind_factor	0.210
cd	0.126
coef_mix_KH	0.097
coef_wind_stir	0.060
ce	0.034
coef_mix_conv	0.015
coef_mix_hyp	0.008

4.3 Simulation results

The calibration of the lake level simulation yields its best fit for the combination of the inflow factors for the defined

20 tributaries River Ammer of 1.10, River Fischbach of 0.72, groundwater of 1.07, and Rivers Rott, Kienbach and all other smaller and unknown inflows of 1.01. By using these adapted inflow factors instead of the default value of 1.0, overall RMSE reduced significantly from 1.10 m to 0.20 m, and the MBE from -1.00 m to 0.09 m, and the achieved model fit can be assessed as very satisfactory. The simulation shows periods of general deviations of over 0.20 m up to 0.55 m for some months, but reproduces well the short-term fluctuations (Fig. 8). The remaining errors and differences can be

25 ascribed to the uncertainties and lack of data for some inflows as assumptions and estimations for the unknown surface input and the groundwater inflow had to be made. More detailed hydrological data might explain remarkable dates, like during summer, when the trend of simulated and observed lake level changes abruptly. No obvious explanation for these trend shifts could be found, although a detailed investigation of the existing hydrological data was conducted. An impact of a highly complex groundwater inflow system is likely to have a key role in the water balance of the lake,

30 which is not considered by the applied input data sufficiently. Furthermore it cannot be ruled out that unknown alterations or errors in the observation setup of the gauges cause these "turning points" as some of them correspond to

flood events, which might have implied problems with the measurements. However, it was possible to improve the lake level simulation distinctively considering only the parameter *inflow_factor* for multiple inflows within the calibration process.
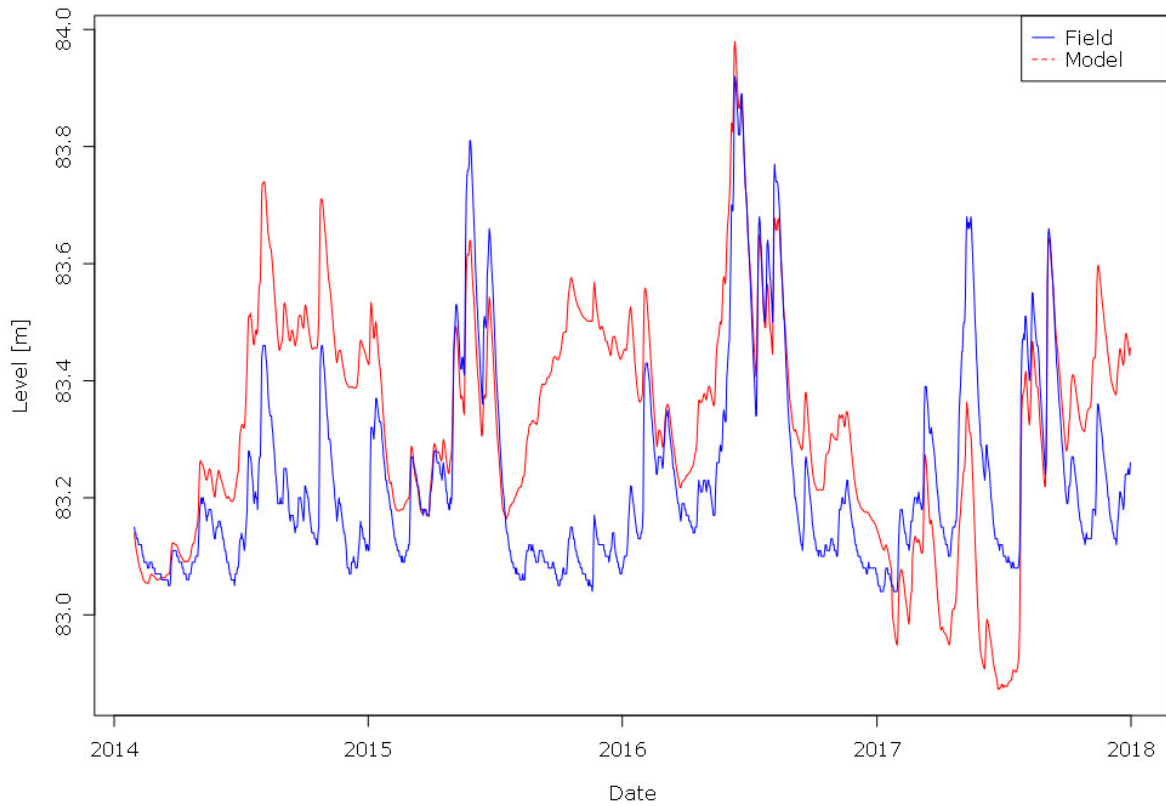
Fig. 8: Observed (blue) and simulated (red) lake level of Lake Ammersee.

Simulated water temperatures reveal an overall RMSE of 1.172 °C. The highest deviations occur within the metalimnion at a depth between 7 – 18 m (Bueche and Vetter, 2014b) during summer stratification, when the model underestimates the temperature (Fig. 9). This is accompanied by too warm layers in the upper epilimnion in a depth of about 20 m. However, the general seasonal pattern is reproduced adequately and differences during winter are negligible.
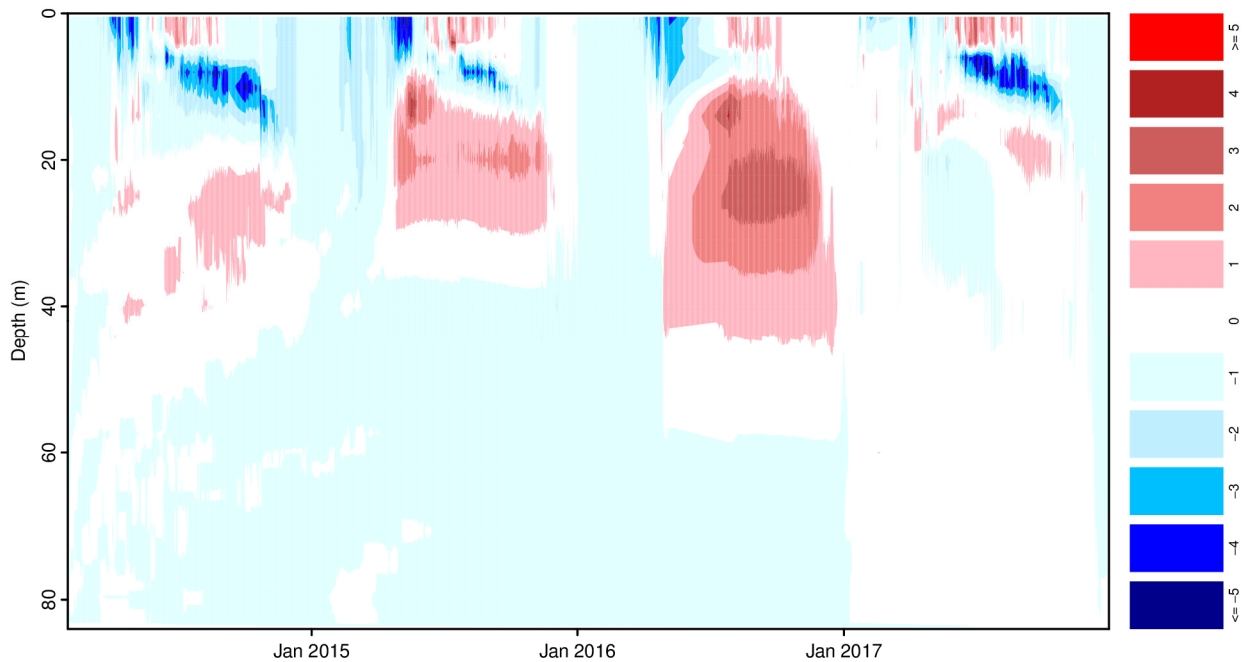
13

Fig. 9: Contour plot of differences between simulated and observed water temperatures of Lake Ammersee.

5 Discussion

The implemented option of an autocalibration in the toolbox enables a less time-consuming and more efficient
5 parameter optimization compared to a conventional manual calibration procedure (Luo et al., 2018). The utilization of
such automatization techniques is advised for lake modeling studies (Ladwig et al., 2018). Hence, the provided tool can
be seen as the centerpeace of the developed GLM Toolbox, which is complemented by the plotting option of differences
between observed and simulated water temperatures. This model output visualization enables an immediate overview
on the simulated deviations and their spatial distribution without any further post-processing of the model results.
10 Although no detailed quantification of the error is possible, this illustration allows a very quick qualitative comparison
of different simulation settings. Such visualization option for GLM output has not yet been provided for an open-source
software before.

The easy handling and free availability of the GUI expands the reach to potential user of the GLM beyond the
limnological research specialists. The used scripting language R is already widespread in limnological (e.g. Winslow et
15 al., 2016), hydrological and environmental research (e.g. Pilz et al., 2017; Gampe et al., 2016), as well as in the field of
automation of water management processes (e.g. Erban et al., 2018). Providing the R code as development version
(http://doi.org/10.5281/zenodo.2025865) in addition to the R package, enabling the GUI and its tools to be easily
customized by users for other specific demands and then again to be shared with the public.

Due to the small number of considered parameters in the calibration process of the presented case studies, the efficiency
20 was successfully tested for a realistic effort of time. The visibility of the simulation error provided by the created
difference contour plots gives the opportunity to combine the automated calibration easily with expert knowledge.
However, the time consumption of an autocalibration run of several days and more for combinations of larger number
of parameters and higher intervals might hamper of the calibration efficiency of a solely automatized calibration and
can be improved in upcoming versions of the toolbox. At present running the tool on a server in advance or as a
25 "background task" can compensate for this problem.

Further limitations of the toolbox/GUI have to be mentioned and more coding activities should be addressed to
minimize the following issues. 1) The contour plots of water temperatures indicate the lake level on the bottom either

interpolated or in very coarse lake level fluctuation, which does not allow a sufficient derivation of this model output by these plots. For this purpose separated plots of the lake level simulations can be created. 2) The calibration algorithm of the toolbox creates parameter values with a high decimal precision due to the approach of percental alteration. This might pretend a false sensitivity of the model and a too detailed accuracy of the calibration for the respective parameter.

5 3) The method of the sensitivity analysis will yield a SI = 0 for any included parameter with the initial value being 0. This applies for example to *seepage_rate* as its default value is 0. 4) The applied model version of GLM is dependent of the maintenance on the R package *glmtools*.

The presented simulations of lake water temperatures have an average overall RMSE of 1.30 °C and 1.17 °C. This is within the range of values obtained by other lake modeling studies applying GLM or other lake 1-D models (Bueche et

10 al., 2017; Ladwig et al., 2018; Robertson et al., 2018; Frassl et al., 2018). This simulation quality was achieved even by only a few autocalibration runs showing the effectiveness of the tool.

In addition to the visualization options and the calibration tool for water temperature simulations, *glmGUI* enables also a calibration of the lake level to achieve a correct reproduction of the water stage. This is especially important for smaller lakes, for which an incorrect simulation of the lake level can have a significant impact on the water temperature

15 reproduction. Furthermore, as the lake level is the result of the lake-catchment water balance (Vanderkelen et al., 2018), the applicability of GLM is enhanced also to hydrological analysis and water balance investigations by this feature. The GLM uses the bulk aerodynamic formula to estimate the latent heat flux and therefore evaporation (Hipsey et al., 2014), which is commonly applied to assess the evaporation rate over open water bodies (Fischer et al., 1979; Hicks, 1972). Including the GLM in the hydrological analysis can therefore improve the accuracy of the modeled evaporation and

20 thus the water balance estimate. In this study, a RMSE for the lake level simulations of 0.11 m (Lake Baratz) and 0.20 m (Lake Ammersee) is achieved, which is within the range of the GLM performance shown by Weber et al. (2017), and attests a good accordance of the modeled water level with the observed values (Hostetler, 1990).

The GUI is also able to execute simulation runs of GLM coupled with water quality models of ecological lake models (e.g. Aquatic Ecodynamics Modelling Library, AED). Although water quality settings cannot yet be changed using the

25 toolbox, any model generated output can be plotted.

5 Conclusions

The presented R package *glmGUI* wraps up simulation and processing tools for the GLM. This includes a tool to autocalibrate the model and options of a parameter sensitivity analysis. Both tools can be used to examine the two simulation output variables of water temperature and lake level. Furthermore, *glmGUI* implements several

30 visualizations options for the meteorological and hydrological input data and the model output. After the deployment of other R packages to execute GLM and for model output post-processing and statistical analysis (*rLakeAnalyzer*, *rGLM*, *glmtools*) *glmGUI* close the gap of missing tools to simplify and accelerate the calibration process and to extend visualization options.

The tools are tested for two different lakes (deep, dimictic, perennial inflow, and shallow, monomictic, seasonal inflow)

35 located in varying climate zones. Good model results were achieved after a low expenditure of calibration effort. In contrast to many other studies an exhaustive description of the simulation input data and field data (data for Lake Ammersee also provided as example data) is given within this paper (as Supplemetal Material). The GUI includes tools to check the quality of the input data. This comprises the option of a visual detection of errors, missing values and plausibility.

The development of *glmGUI* for the free and open-source programming language R, available on all common platforms (Windows, OS X, Linux), makes it accessible for anyone to use, which contributes to scientific transparency (Winslow et al., 2018). The GUI allows a high level of interoperability due to the option of combining with other operating systems. This includes the coupling of GLM with ecological lake models (e.g. Snortheim et al., 2017; Robertson et al., 2018; Weber et al., 2017; Fenocchi et al., 2019), as the toolbox is already applicable for this purpose and can be the basis for establishing of a coupling interface. Furthermore, we designed the software with the aim of a high flexibility for the application of other scenarios, for various study areas or with diverse time steps. An increasing number of lake modeling studies are investigating the impact of global change on lakes using as meteorological input data regional climate model output or future scenarios (Fenocchi et al., 2018; Weinberger and Vetter, 2014; Bueche and Vetter, 2015; Ladwig et al., 2018; Pietikäinen et al., 2018; Piccolroaz and Toffolon, 2018). For analyses in these fields of research the presented R package *glmGUI* will be a powerful tool, especially concerning the provided difference contour plots.

Code and data availability: The package and R-code are available at http://doi.org/10.5281/zenodo.2025865. Example data for Lake Ammersee are attached to this paper as a supplementary data. Sources are described in Supplementary Material, section 2Appendix B.

Appendix A: Model input data and calibration parameter

Table A1: Required model input data (after Hipsey et al., 2014).

Parameter	Unit	Description
Meteorological parameters:		
Air temperature	°C	average air temperature 10 m above the water surface
Wind speed	ms^{-1}	average wind speed 10 m above the water surface
Relative Humidity	%	average relative humidity (0 – 100 %) 10 m above the water surface
Shortwave radiation	Wm^{-2}	average shortwave radiation
Longwave radiation	Wm^{-2}	Longwave radiation input is assumed to be direct incident intensity
Rainfall	md^{-1}	rainfall depth
Cloud cover *(optional)*	-	Required if no information on longwave radiation available and incoming longwave flux is estimated from cloud cover fraction data
Snowfall *(optional)*	md^{-1}	snowfall depth
Hydrological parameters:		
Inflow discharge	m^3s^{-1}	Average discharge
Water temperature	°C	average streamflow water temperature
Salinity *(optional)*	mgl^{-1}	streamflow salinity
Outflow discharge	m^3s^{-1}	average discharge

Table A2: List of preselected parameters for autocalibration (after Hipsey et al., 2017).

Parameter (glm.nml ID)	Description
Lake Properties	
Kw	Extinction coefficient for PAR radiation (unit: m^{-1})
Surface Dynamics	
ch	Bulk aerodynamic coefficient for sensible heat transfer
ce	Bulk aerodynamic coefficient for latent heat transfer
cd	Bulk aerodynamic coefficient for transfer of momentum
Mixing Parameters	
coef_mix_conv	Mixing efficiency - convective overturn
coef_wind_stir	Mixing efficiency - wind stirring
coef_mix_shear	Mixing efficiency - shear production
coef_mix_turb	Mixing efficiency - unsteady turbulence (acceleration)
coef_mix_KH	Mixing efficiency - Kelvin-Helmholtz turbulent billows
coef_mix_hyp	Mixing efficiency of hypolimnetic turbulence
Hydrological and meteorological factors	
seepage_rate	Rate of seepage from the deepest layer (unit: m day^{-1})
inflow_factor	Factor for inflow(s)
outflow_factor	Factor for outflow
Rain_factor	Factor for rainfall
wind_factor	Factor for wind speed

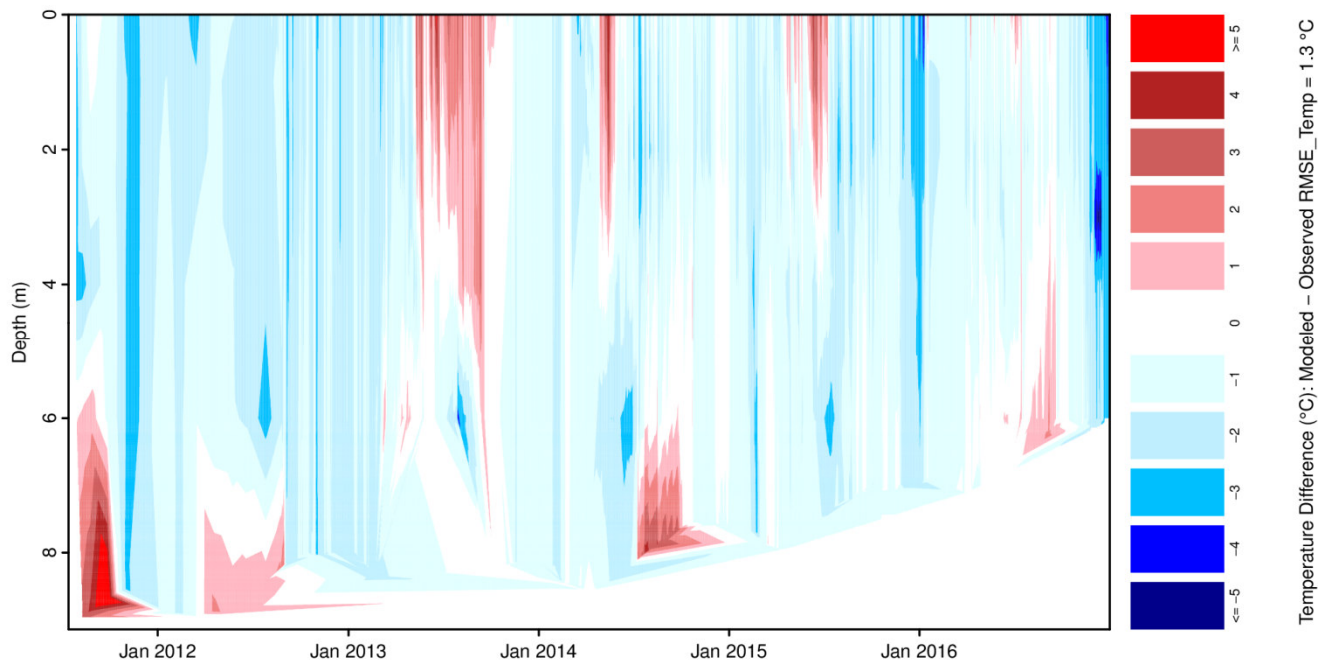## Appendix B: Contour plot of GLM simulations

Fig. B1: Contour plot of differences between simulated and observed water temperatures of Lake Baratz.

References

5   Bay. LfU, Bayerisches Landesamt für Umwelt: Gewässerkundlicher Dienst Bayern, https://www.gkd.bayern.de/, 2018

Bruce, L. C., Frassl, M. A., Arhonditsis, G. B., Gal, G., Hamilton, D. P., Hanson, P. C., Hetherington, A. L., Melack, J. M., Read, J. S., Rinke, K., Rigosi, A., Trolle, D., Winslow, L., Adrian, R., Ayala, A. I., Bocaniov, S. A., Boehrer, B., Boon, C., Brookes, J. D., Bueche, T., Busch, B. D., Copetti, D., Cortés, A., de Eyto, E., Elliott, J. A., Gallina, N., Gilboa, Y., Guyennon, N., Huang, L., Kerimoglu, O., Lenters, J. D., MacIntyre, S., Makler-Pick, V., McBride, C. G., Moreira, S., Özkundakci, D., Pilotti, M., Rueda, F. J.,
10   Rusak, J. A., Samal, N. R., Schmid, M., Shatwell, T., Snorthheim, C., Soulignac, F., Valerio, G., van der Linden, L., Vetter, M., Vinçon-Leite, B., Wang, J., Weber, M., Wickramaratne, C., Woolway, R. I., Yao, H., and Hipsey, M. R.: A multi-lake comparative analysis of the General Lake Model (GLM): Stress-testing across a global observatory network, Environmental Modelling & Software, 102, 274-291, https://doi.org/10.1016/j.envsoft.2017.11.016, 2018.

Bucak, T., Trolle, D., Tavşanoğlu, Ü. N., Çakıroğlu, A. İ., Özen, A., Jeppesen, E., and Beklioğlu, M.: Modeling the effects of
15   climatic and land use changes on phytoplankton and water quality of the largest Turkish freshwater lake: Lake Beyşehir, Science of The Total Environment, 621, 802-816, https://doi.org/10.1016/j.scitotenv.2017.11.258, 2018.

Bueche, T., and Vetter, M.: Influence of groundwater inflow on water temperature simulations of Lake Ammersee using a one-dimensional hydrodynamic lake model, Erdkunde, 68, 19-31, 10.3112/erdkunde.2014.01.03 2014a.

Bueche, T., and Vetter, M.: Simulating water temperatures and stratification of a pre-alpine lake with a hydrodynamic model:
20   calibration and sensitivity analysis of climatic input parameters, Hydrological Processes, 28, 1450-1464, 10.1002/hyp.9687, 2014b.

Bueche, T., and Vetter, M.: Future alterations of thermal characteristics in a medium-sized lake simulated by coupling a regional climate model with a lake model, Climate Dynamics, 44, 371-384, 10.1007/s00382-014-2259-5, 2015.

Bueche, T.: The mixing regime of Lake Ammersee, DIE ERDE–Journal of the Geographical Society of Berlin, 147, 275-283, 10.12854/erde-147-24, 2016.

25   Bueche, T., Hamilton, D. P., and Vetter, M.: Using the General Lake Model (GLM) to simulate water temperatures and ice cover of a medium-sized lake: a case study of Lake Ammersee, Germany, Environmental Earth Sciences, 76, 10.1007/s12665-017-6790-7, 2017.

Carey, C. C., and Gougis, R. D.: Simulation modeling of lakes in undergraduate and graduate classrooms increases comprehension of climate change concepts and experience with computational tools, Journal of Science Education and Technology, 26, 1-11, 2017.

30   Chapra, S. C.: Surface water-quality modeling, Waveland press, 2008.

Erban, L. E., Balogh, S. B., Campbell, D. E., and Walker, H. A.: An R Package for Open, Reproducible Analysis of Urban Water Systems, With Application to Chicago, Open Water Journal, 5, 2018.

Fenocchi, A., Rogora, M., Sibilla, S., and Dresti, C.: Relevance of inflows on the thermodynamic structure and on the modeling of a deep subalpine lake (Lake Maggiore, Northern Italy/Southern Switzerland), Limnologica-Ecology and Management of Inland
35   Waters, 42-56, 10.1016/j.limno.2017.01.006, 2017.

Fenocchi, A., Rogora, M., Sibilla, S., Ciampittiello, M., and Dresti, C.: Forecasting the evolution in the mixing regime of a deep subalpine lake under climate change scenarios through numerical modelling (Lake Maggiore, Northern Italy/Southern Switzerland), Climate Dynamics, 1-16, 2018.

5   Fenocchi, A., Rogora, M., Morabito, G., Marchetto, A., Sibilla, S., and Dresti, C.: Applicability of a one-dimensional coupled ecological-hydrodynamic numerical model to future projections in a very deep large lake (Lake Maggiore, Northern Italy/Southern Switzerland), Ecological Modelling, 392, 38-51, https://doi.org/10.1016/j.ecolmodel.2018.11.005, 2019.

Fischer, H. B., List, J. E., Koh, C. R., Imberger, J., and Brooks, N. H.: Mixing in Inland and Coastal Waters, Academic Press, 1979.

Frassl, M., Weber, M., and Bruce, L. C.: The General Lake Model (GLM). NETLAKE toolbox for the analysis of high-frequency data from lakes (Factsheet 3). Technical report. NETLAKE COST Action ES1201., 11-15, 2016.

10   Frassl, M., Boehrer, B., Holtermann, P., Hu, W., Klingbeil, K., Peng, Z., Zhu, J., and Rinke, K.: Opportunities and Limits of Using Meteorological Reanalysis Data for Simulating Seasonal to Sub-Daily Water Temperature Dynamics in a Large Shallow Lake, Water, 10, 594, 10.3390/w10050594, 2018.

Gampe, D., Ludwig, R., Qahman, K., and Afifi, S.: Applying the Triangle Method for the parameterization of irrigated areas as input for spatially distributed hydrological modeling — Assessing future drought risk in the Gaza Strip (Palestine), Science of The Total Environment, 543, 877-888, 10.1016/j.scitotenv.2015.07.098, 2016.

15   Giadrossich, F., Niedda, M., Cohen, D., and Pirastru, M.: Evaporation in a Mediterranean environment by energy budget and Penman methods, Lake Baratz, Sardinia, Italy, Hydrology and Earth System Sciences, 19, 2451-2468, 10.5194/hess-19-2451-2015, 2015.

Grewal, M. S.: Kalman filtering, in: International Encyclopedia of Statistical Science, Springer, 705-708, 2011.

Hanson, P. C., Weathers, K. C., and Kratz, T. K.: Networked lake science: how the Global Lake Ecological Observatory Network
20   (GLEON) works to understand, predict, and communicate lake ecosystem response to global change, Inland Waters, 6, 543-554, 2016.

Hicks, B.: Some evaluations of drag and bulk transfer coefficients over water bodies of different sizes, Boundary-Layer Meteorology, 3, 201-213, 1972.

Hipsey, M. R., Bruce, L. C., and Hamilton, D. P.: GLM - General Lake Model: Model overview and user information. AED Report
25   #26, The University of Western Australia Technical Manual, 22, 2014.

Hipsey, M. R., Bruce, L. C., Boon, C., Busch, B., Carey, C. C., Hamilton, D. P., Hanson, P. C., Read, J. S., de Sousa, E., Weber, M., and Winslow, L. A.: A General Lake Model (GLM 2.4) for linking with high-frequency sensor data from the Global Lake Ecological Observatory Network (GLEON), Geoscientific Model Development Discussions, 1-60, 10.5194/gmd-2017-257, 2017.

Hipsey, M. R., Bruce, L. C., Boon, C., Busch, B., Carey, C. C., Hamilton, D. P., Hanson, P. C., Read, J. S., de Sousa, E., Weber, M.,
30   and Winslow, L. A.: A General Lake Model (GLM 3.0) for linking with high-frequency sensor data from the Global Lake Ecological Observatory Network (GLEON), Geosci. Model Dev., 12, 473-523, 10.5194/gmd-12-473-2019, 2019.

Holmes, R. W.: The Secchi Disk in turbid Costal Waters, Limnology and oceanography, 15, 688-694, 1970.

Hornung, R.: Numerical Modelling of Stratification in Lake Constance with the 1-D hydrodynamic model DYRESM, University of Stuttgart, Stuttgart, 101 pp., 2002.

35   Hostetler, S. W.: Simulation of Lake Evaporation With Aoolication to Modeling Lake Level Variations of Harney-Malheur Lake, Oregon, Water Resources Research, 26, 2603-2612, 1990.

Hyndman, R. J., and Khandakar, Y.: Automatic time series for forecasting: the forecast package for R, 6/07, Monash University, Department of Econometrics and Business Statistics, 2007.

Ladwig, R., Furusato, E., Kirillin, G., Hinkelmann, R., and Hupfer, M.: Climate Change Demands Adaptive Management of Urban
40   Lakes: Model-Based Assessment of Management Scenarios for Lake Tegel (Berlin, Germany), Water, 10, 186, 10.3390/w10020186, 2018.

Lenhart, T., Eckhardt, K., Fohrer, N., and Frede, H.-G.: Comparison of two different approaches of sensitivity analysis, Physics and Chemistry of the Earth, Parts A/B/C, 27, 645-654, 2002.

Luo, L., Hamilton, D., Lan, J., McBride, C., and Trolle, D.: Autocalibration of a one-dimensional hydrodynamic-ecological model
45   (DYRESM 4.0-CAEDYM 3.1) using a Monte Carlo approach: simulations of hypoxic events in a polymictic lake, Geoscientific Model Development, 11, 903-913, 2018.

Mi, C., Frassl, M. A., Boehrer, B., and Rinke, K.: Episodic wind events induce persistent shifts in the thermal stratification of a reservoir (Rappbode Reservoir, Germany), International Review of Hydrobiology, 103, 71-82, 10.1002/iroh.201701916, 2018.

Niedda, M., and Pirastru, M.: Hydrological processes of a closed catchment-lake system in a semi-arid Mediterranean environment,
50   Hydrological Processes, 27, 3617-3626, 10.1002/hyp.9478, 2013.

Niedda, M., Pirastru, M., Castellini, M., and Giadrossich, F.: Simulating the hydrological response of a closed catchment-lake system to recent climate and land-use changes in semi-arid Mediterranean environment, Journal of Hydrology, 517, 732-745, http://dx.doi.org/10.1016/j.jhydrol.2014.06.008, 2014.

Pianosi, F., Beven, K., Freer, J., Hall, J. W., Rougier, J., Stephenson, D. B., and Wagener, T.: Sensitivity analysis of environmental
55   models: A systematic review with practical workflow, Environmental Modelling & Software, 79, 214-232, https://doi.org/10.1016/j.envsoft.2016.02.008, 2016.

Piccolroaz, S., and Toffolon, M.: The fate of Lake Baikal: how climate change may alter deep ventilation in the largest lake on Earth, Climatic Change, 150, 181-194, 2018.

Pietikäinen, J.-P., Markkanen, T., Sieck, K., Jacob, D., Korhonen, J., Räisänen, P., Gao, Y., Ahola, J., Korhonen, H., and Laaksonen, A.: The regional climate model REMO (v2015) coupled with the 1-D freshwater lake model FLake (v1): Fenno-Scandinavian climate and lakes, Geoscientific Model Development, 11, 2018.

Pilz, T., Francke, T., and Bronstert, A.: lumpR 2.0. 0: an R package facilitating landscape discretisation for hillslope-based hydrological models, 2017.

Pirastru, M., and Niedda, M.: Evaluation of the soil water balance in an alluvial flood plain with a shallow groundwater table, Hydrological Sciences Journal, 58, 898-911, 10.1080/02626667.2013.783216, 2013.

Poole, H., and Atkins, W.: Photo-electric measurements of submarine illumination throughout the year, Journal of the Marine Biological Association of the United Kingdom, 16, 297-324, 1929.

Rigosi, A., Marcé, R., Escot, C., and Rueda, F. J.: A calibration strategy for dynamic succession models including several phytoplankton groups, Environmental Modelling & Software, 26, 697-710, 10.1016/j.envsoft.2011.01.007, 2011.

Robertson, D. M., Juckem, P. F., Dantoin, E. D., and Winslow, L. A.: Effects of water level and climate on the hydrodynamics and water quality of Anvil Lake, Wisconsin, a shallow seepage lake, Lake and Reservoir Management, 1-21, 10.1080/10402381.2017.1412374, 2018.

Snortheim, C. A., Hanson, P. C., McMahon, K. D., Read, J. S., Carey, C. C., and Dugan, H. A.: Meteorological drivers of hypolimnetic anoxia in a eutrophic, north temperate lake, Ecological Modelling, 343, 39-53, 2017.

Vanderkelen, I., van Lipzig, N. P., and Thiery, W.: Modelling the water balance of Lake Victoria (East Africa), part 1: observational analysis, Hydrol. Earth Syst. Sci, discussion, 2018.

Verzani, J.: Examples for gWidgets, R package version gWidgets 0.0-41, https://cran.r-project.org/web/packages/gWidgets/vignettes/gWidgets.pdf, 2014

Vetter, M., and Sousa, A.: Past and current trophic development in Lake Ammersee - Alterations in a normal range or possible signals of climate change?, Fund Appl Limnol, 180, 41-57, 10.1127/1863-9135/2012/0123, 2012.

Weber, M., Rinke, K., Hipsey, M. R., and Boehrer, B.: Optimizing withdrawal from drinking water reservoirs to reduce downstream temperature pollution and reservoir hypoxia, Journal of Environmental Management, 197, 96-105, https://doi.org/10.1016/j.jenvman.2017.03.020, 2017.

Weinberger, S., and Vetter, M.: Lake heat content and stability variation due to climate change: coupled regional climate model (REMO)-lake model (DYRESM) analysis, Journal of Limnology, 73, 93-105, 10.4081/jlimnol.2014.668, 2014.

Williamson, C. E., Saros, J. E., and Schindler, D. W.: Sentinels of Change, Science, 323, 887-888, 10.1126/science.1169443, 2009.

Winslow, L., Read, J., Woolway, R. I., Brentrup, J., Leach, T., and Zwart, J.: rLakeAnalyzer: 1.8.3 Standardized methods for calculating common important derived physical features of lakes 2016

Winslow, L. A., Zwart, J. A., Batt, R. D., Dugan, H. A., Woolway, R. I., Corman, J. R., Hanson, P. C., and Read, J. S.: LakeMetabolizer: an R package for estimating lake metabolism from free-water oxygen using diverse statistical models, Inland Waters, 6, 622-636, 10.1080/iw-6.4.883, 2018.

speeds measured at the lake station were 1.19 ms^{-1} (average difference) lower than measured at Fertilia station. After the 21.06.2016 the average difference was only 0.08 ms^{-1}. Observations at Grifone station are within the range of the measurements taken at the lake station before 21.06.2016, hence these data were taken as reference for correction.
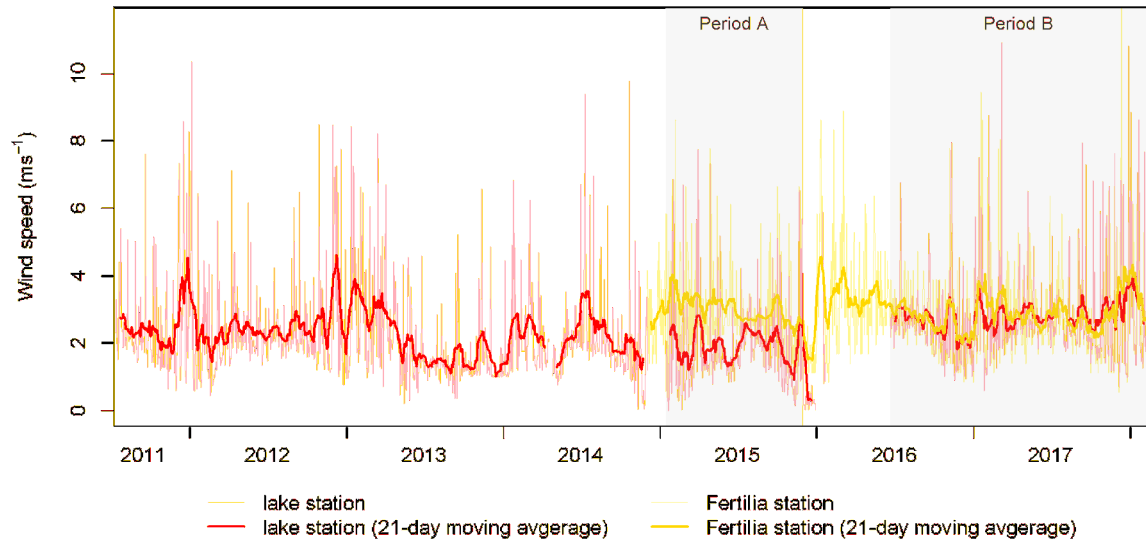

Fig. S2: Time series of daily wind speeds at lake and Fertilia station. Periods A and B are used for mean value comparison (see Table S1)

Table S1: Averages of wind speed at lake and Fertilia station

Period	lake station	Fertilia station
15.01.2015 - 30.12.2015 (period A, Fig. S2)	1.82	3.01
21.06.2016 - 12.02.2018 (period B, Fig. S2)	2.71	2.79

The final time series of wind speed input data (daily values) were prepared first by filling gaps of observations by linear correlation (Table S2), and secondly by adjusting of the values after the 21.06.2016 by multiplying with the factor of 0.67, which is equal to the quotient of the average data for periods before and after at the raft station (see Table S1).

Table S2: Gaps of observations for wind speed at the lake station, station from which data were used, and coefficient of correlation

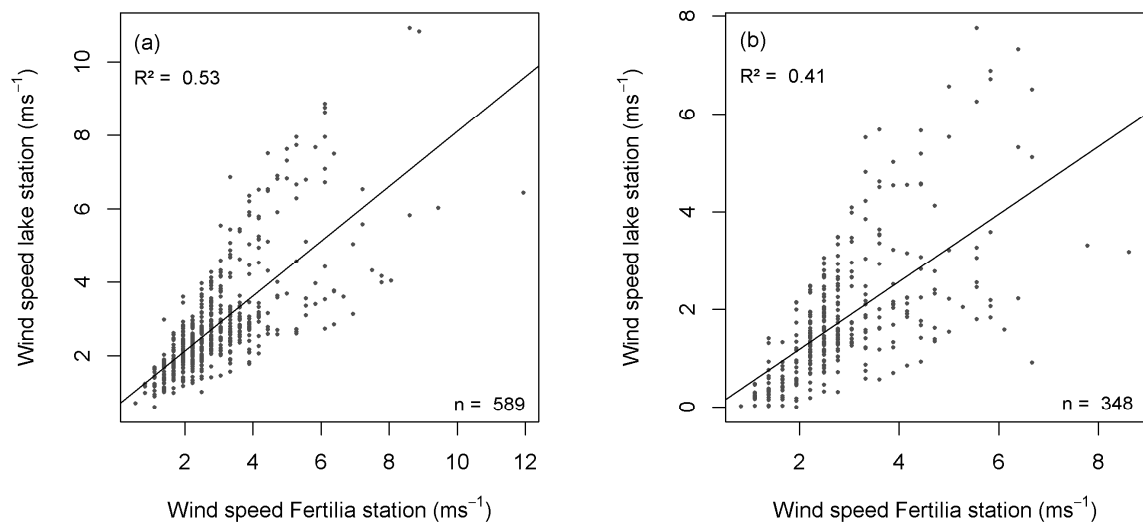| Period of data gap	Data source	Reference period	R²	Comment
24.09.2013 – 24.04.2014	Grifone	08.07.2011 – 23.09.2013	0.72	(Giadrossich et al., 2015)
04.12.2014 – 14.01.2015	Fertilia	21.06.2016 – 12.02.2018	0.53	see Fig. S3a
31.05.2015 – 20.06.2016	Fertilia	15.01.2015 – 30.12.2015	0.41	see Fig. S3b

Fig. S3: Linear correlation of wind speed for the lake and Fertilia station, a) period 21.06.2016 to 11.02.2018, b) 15.01.2015 to 30.12.2015

S1.2.3 Relative humidity

Missing data for the lake station were filled by linear correlation. Table S3 gives an overview on the interpolated gaps and the used data source. The maximum observed value for relative humidity at the lake station is 96.89 %. Values computed from the other stations may exceed this value and were then set to be 97.0 %.

Table S3: Gaps of observations for relative humidity at the lake station, station from which data were used, and coefficient of correlation

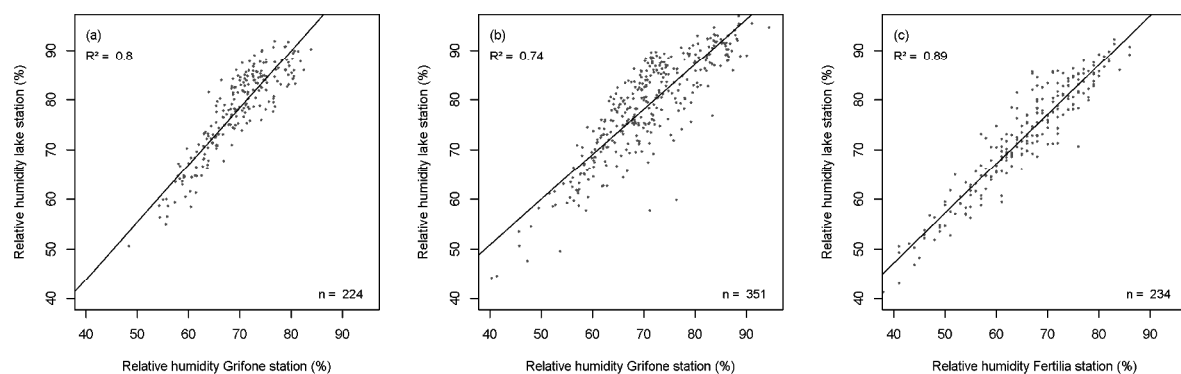| Period of data gap	Data source	Reference period	R^2	Comment
24.09.2013 – 24.04.2014	Grifone	08.07.2011 – 23.09.2013	0.82	(Giadrossich et al., 2015)
04.12.2014 – 14.01.2015	Grifone	24.04.2014 – 03.12.2014	0.80	see Fig. S4a
21.01.2016 – 22.03.2016	Grifone	08.10.2015 – 23.11.2016	0.74	see Fig. S4b
24.11.2016 – 22.03.2017	Fertilia	24.03.2017 – 20.11.2017	0.89	see Fig. S4c

Fig. S4: Linear correlation of relative humidity for the lake station and Grifone station (a) period 24.04.2014 – 03.12.2014 and b) period 08.10.2015 – 23.11.2016) and c) Fertilia station.

3

S1.2.4 Rainfall

No precipitation data are obtained at the lake station. Measurements exist at Grifone site until 31.05.2017. Table S4 shows the gaps in the rainfall time series at Grifone station and the source for filling.

Table S4: Gaps of observations for rainfall at Grifone and information on filling method

Period of data gap	Number of days	Data source (rainfall data)	Filling method/comment
18.08.2013 – 23.08.2013	6	-	assumed to be 0
14.09.2015 – 07.10.2015	24	-	Estimated from soil moisture data at Grifone station
28.11.2016 – 10.12.2016	13	Olmedo & Capo Caccia	Average of the two stations
15.12.2016 – 20.12.2016	6	Olmedo & Capo Caccia	Average of the two stations
12.01.2017 – 09.03.2017	57	Olmedo & Capo Caccia	Average of the two stations
10.03.2017 – 22.03.2017	13	*Not filled*	
01.06.2017 – 31.08.2017	92	-	Assumed to be 0
01.09.2017 – 12.02.2018	193	Capo Caccia	

The mean annual precipitation at Grifone is about 600 mm (Pirastru and Niedda, 2013) and Sardinia is characterized by a rainy winter season and dry summer months (Niedda et al., 2014; Chessa et al., 1999). Hence, periods in summer with no rainfall observations are assumed to be 0.

S1.2.5 Shortwave and longwave radiation

Radiation measurements representing the net radiation are available at lake station and Grifone station. All data gaps at the lake station are filled by linear correlation from Grifone (R^2 = 0.93, Fig. S5). Three short gaps with maximum of eight days are filled by linear interpolation. The required (incoming) shortwave R_{Sin} (Wm^{-2}) and longwave (net) radiation R_{Lnet} (Wm^{-2}) are calculated from the net radiation values using the energy balance:

$$R_n = (1 - \alpha) * R_{sin} + R_{Lnet} \tag{1}$$

where R_n is the net radiation (Wm^{-2}), α is the albedo of the water surface (assumed to be 0.2, Hipsey et al., 2014). Net longwave is described as (Hipsey et al., 2017):

$$R_{Lnet} = R_{Lin} - R_{Lout} \tag{2}$$

where R_{Lout} (Wm^{-2}) is the outgoing longwave radiation and R_{Lin} (Wm^{-2}) is the incoming radiation. Based on the Stefan-Boltzmann law the incoming and outgoing longwave can be calculated from the emissivity and temperature of water and air, respectively (An et al., 2017):

$$R_{Lout} = \varepsilon_w * \sigma * (T_s + 273.1)^4 \tag{3}$$

$$R_{Lin} = \varepsilon_a * \sigma * (T_a + 273.1)^4 \tag{4}$$

where ε_W the emissivity of the water surface, assumed to be 0.985 (Hipsey et al., 2017), ε_a is the air emissivity, σ is the Stefan-Boltzman constant, T_S is the surface water temperature (°C), and T_a is the air temperature (°C). For T_s measurements from the lake surface can be used. For days with no observations T_s is calculated from T_a by polynomial regression (R^2 = 0.88, Fig. S6~~Fig. S6~~):

$$y = -6.154 * 10^{-7} * x^6 + 7.048 * 10^{-5} * x^5 - 3.139 * 10^{-3} * x^4 + 6.572 * 10^{-2} * x^3 - 0.620 \\ * x^2 + 2.923 * x + 3.536 \tag{5}$$

Air emissivity is calculated using the expression proposed by An et al., (2017, adopted from Idso, 1981):

4

$$\varepsilon_a = 0.7 + 5.95 * 10^{-4} * e_a * e^{(1500*(T_a - 273.1)^{-1})} \tag{6}$$

$$e_a = \frac{RH}{100} * e_s \tag{7}$$

$$e_s = 0.6107 * e^{17.269*T_a*(T_a + 273.1)^{-1}} \tag{8}$$

where e_a is the vapor pressure (kPa), RH is the relative humidity (%) of air, and e_s is the saturated vapor pressure (kPa) at T_a.
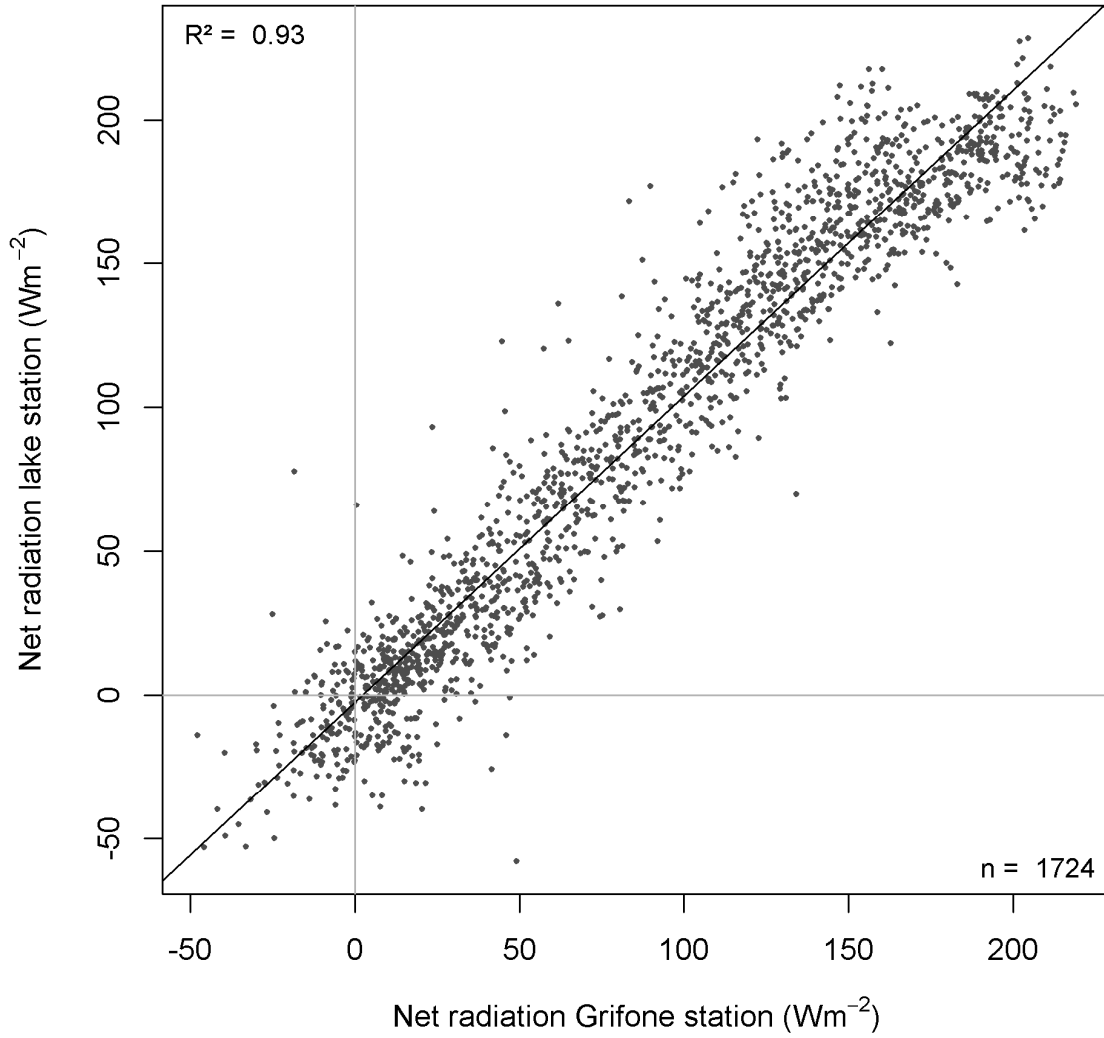

Fig. S5: Linear correlation of net radiation for the lake station and Grifone station (period: 13.07.2011 – 30.05.2017).
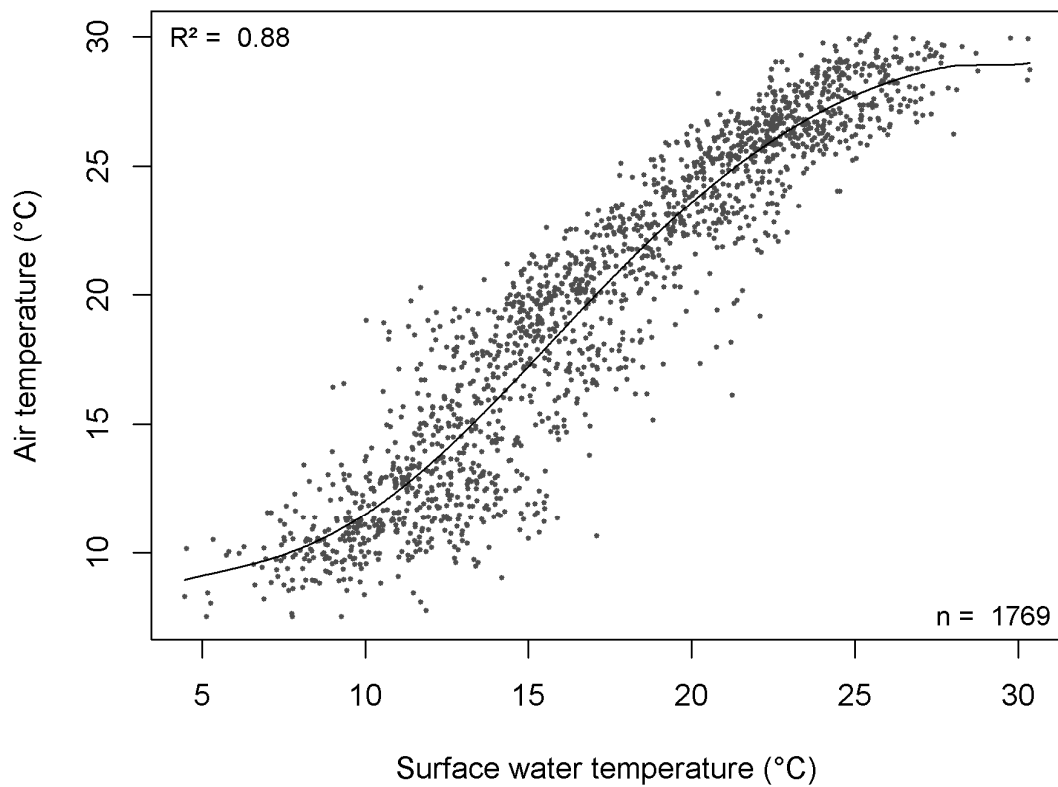
Fig. S6: Polynomial correlation for the surface water and air temperature at the lake station (period: 13.07.2011 – 12.08.2018)

The monthly means of the calculated shortwave radiation exhibit only slight deviations to the values presented by Lavangini et al. (1990, Table S5).

Table S5: Monthly mean of shortwave radiation

month	Shortwave radiation (Wm^{-2})	
	Lavagnini et al. (1990)	calculated
Jan	78.1	91.4
Feb	110.0	120.0
Mar	167.8	181.3
Apr	225.7	242.5
May	289.4	293.4
Jun	312.5	318.9
Jul	312.5	309.2
Aug	277.8	280.4
Sep	223.4	211.3
Oct	148.1	148.3
Nov	81.0	95.3
Dec	67.1	83.0

S1.3 Hydrological model input data

S1.3.1 Inflow discharge

Observed discharge data are available for Grifone site. At the cross-section the sub-catchment area of this gauge is 7.4 km², which represents approximately 62 % of the lake watershed. The inflow to the lake is simulated applying the hydrological model developed by Niedda et al. (2014) representing the entire lake catchment. The daily values of the inflow discharge for the GLM simulation are composed of the observed discharge value of Grifone gauge and 38 % of the simulated discharge representing that percentage of the catchment. Periods without observation data are either set to 0 m³s⁻¹ during dry seasons or filled based on expert knowledge considering rainfall data (24.01.2014 – 12.02.2014).

S1.3.2 Inflow water temperature

Observations of inflow water temperature exist only at Grifone gauge (see Fig. 3, main paper) for the periods 01.10.2015 – 13.05.2017 and 01.01.2017 – 06.07.2017. Values for periods with no observation data are calculated from the air temperature by subtracting 1.0 °C from the daily mean value of air temperature. The computation by linear correlation was discarded, because the time series of water and air temperature show distinctive different relationships for the two applicable periods (with constant stream runoff, Table S6Table S6).

Table S6: Coefficient of correlation and linear relationship for water and air temperature for periods with constant runoff

Period	R²	Linear relationship
27.02.2016 – 13.05.2016	0.29	y = 0.535x + 7.691
17.02.2017 – 11.05.2017	0.84	y = 1.165x - 1.021

S1.3.2 Outflow discharge

The lake has no surface outflow, but an exfiltration to groundwater can be assumed. Niedda et al. (2014) estimate a seepage value of 1.5 mm per day, which is represented by a constant outflow time series in the input data. The average lake surface area of 0.38 km² for the period of July 2011 to August 2017 is applied to calculate the outflow discharge value of 0.0066 ms⁻¹.

S1.4 Lake field data

S1.4.1 Lake level

Lake level data surveyed by means of a diver sensor placed on the lake bottom (further details on the instrument setup see Giadrossich et al. (2015)) with an hourly resolution starting from 18.11.2011. Prior to this date manually measurements are available in a weekly to biweekly resolution. Data from the diver are outputted as height (m) over the lake bottom. The position of the data logger at the lake bottom and thereby its elevation above sea level slightly changes with each re-installation after a data export on the surface. Hence, the data are corrected to refer all heights to the same elevation of 18.85 m a.s.l.. The data taken from the surface are also set to this reference elevation.

S1.4.2 Lake water temperature

Water temperature data were observed automatically by the lake station and are available from 26.08.2012 measuring in the depths of 1, 2, 4, and 6 m in hourly resolution. The surface and bottom water temperature were measured by a diver with an observation start on 26.07.2012 and 23.08.2012, respectively (for further details on the instrument setup see Giadrossich et al. (2015)). From 27.11.2015 also the depths of 3 and 5 m were studied. Prior to the automatically observations temperature profiles were collected manually every 2 to 5 weeks. Fig. S7Fig. S7 visualizes the available filed data of lake water temperature. For the period of 24.09.2013 – 04.03.2014, when the lake station was not in operation (including the diver at the surface), the surface temperature is derived from the bottom temperature based on the assumption of isothermal conditions in the vertical lake profile. Homothermy is common for the site in this season of the year and the vertical temperature gradient of 0.91 °C on 24.09.2014 was already low indicating no stable thermal stratification.
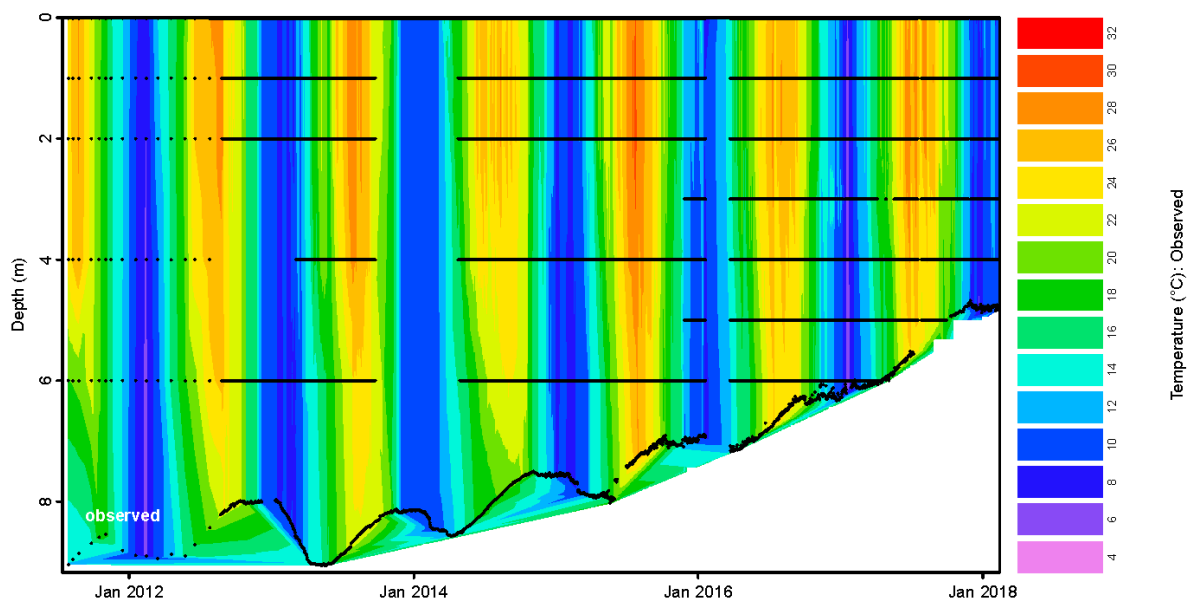

Fig. S7: Visualization of available field data of water temperature (black dots) and interpolated temperatures in the vertical profile (glmGUI).

S2 Input data for Lake Ammersee

S2.1 Observation stations

The locations of hydrological gauging stations (discharge and groundwater) are displayed in Fig. 7 in the main text. Meteorological observation stations are shown in (Fig. S8). Lake field data are surveyed at the Lake station, where also meteorological observations are taken. All data except for cloud cover data (see chapter S.2.2B2) are freely available at https://www.gkd.bayern.de/ provided by the Bavarian Environment Agency (Bay. LfU, 2018).
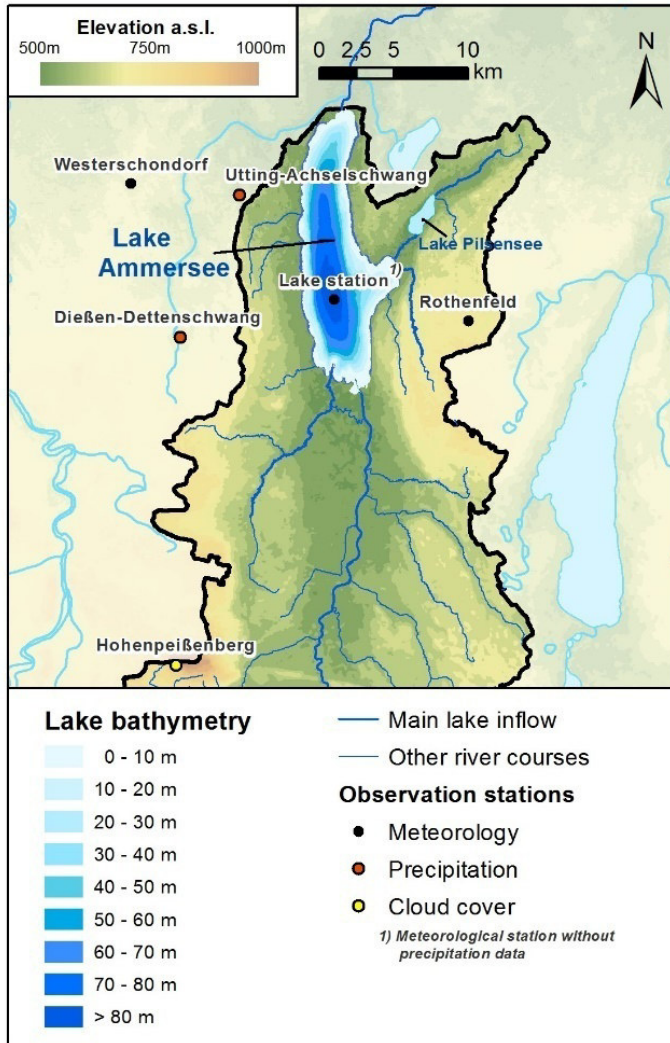
Fig. S8: Bathymetry of Lake Ammersee and meteorological observation stations (Source DEM: Elevation data from ASTER GDEM, a product of METI and NASA, Source geo-data: Geobasisdaten © Bayerische Vermessungsverwaltung, www.geodaten.bayern.de).

S2.2 Meteorological model input data

Observations of air temperature, wind speed, relative humidity, and shortwave radiation are gathered at the lake station as meteorological input data for the simulation. The parameters are measured in a temporal resolution of 15 minutes. Shortwave radiation data are added to daily sums. For the other three parameters daily averages are calculated.

Missing values for wind speed, air temperature and relative humidity are calculated from observations (hourly values) of Rothenfeld station (Fig. S8). The latter two are subject to considerable seasonal variations in the difference of the measurements between the lake and Rothenfeld station (Fig. S98). Hence, missing values are computed by adding the average deviation for the simulation period of the respective month. The monthly mean values are computed based on a 19-day moving average. Missing data for wind speed are calculated from Rothefeld station observations by adding the mean offest value of the simulation period of -1.3 ms^{-1}. Missing values of shortwave radiation data at the lake station are computed from the average of Rothefeld and Westerschondorf measurements (at both stations hourly observations) and no further error correction is required. Precipitation is inputted to the model as averaged values from observations of the stations Rothefeld, Utting-

9

Achselschwang, and Dießen-Dettenschwang. According to Springer et al. (2015)–, the data are recognized as snow as soon as temperatures are below 1.0 °C.

For Lake Ammersee the GLM option of using cloud cover instead of longwave radiation data is selected. The closest location for cloud cover data is Hohenpeißenberg station (Fig. S8, operator: German Weather Service, free available at http://www.dwd.de/cdc, hourly observations) and daily averages are used without correction.
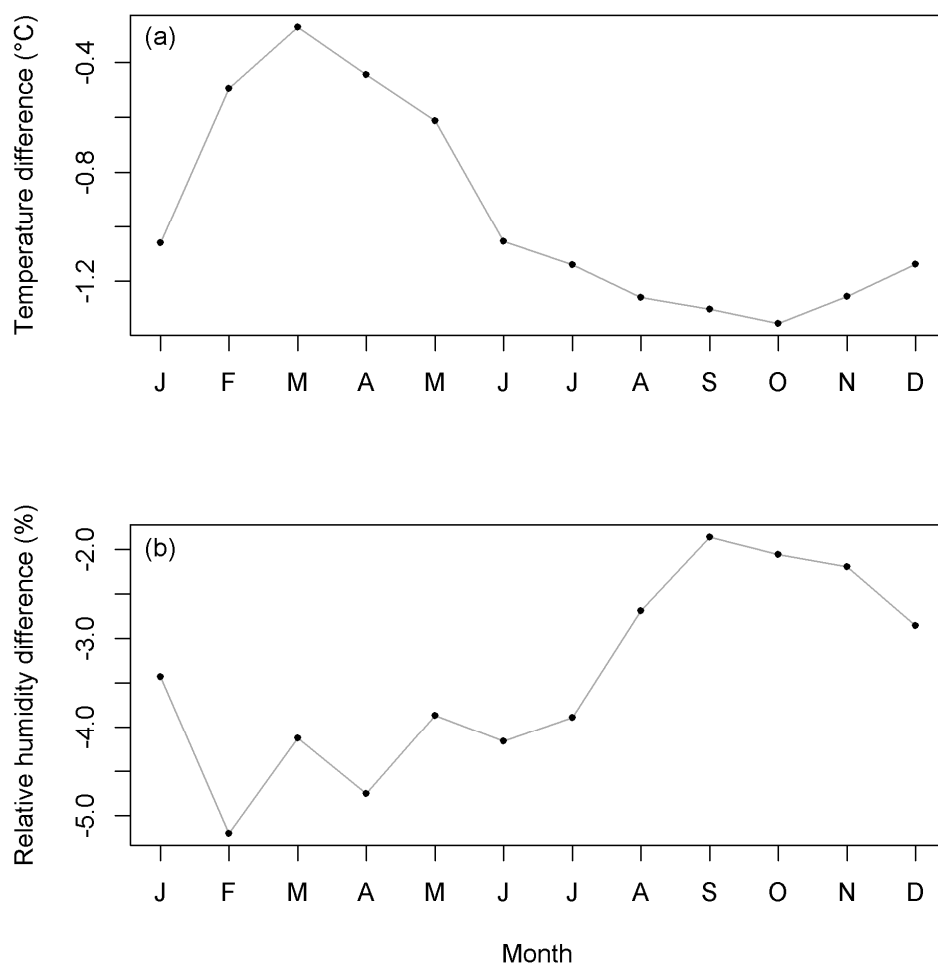

Fig. S9: Average difference (monthly mean of a 19-day moving average) between Rothenfeld and lake station of a) air temperature and b) relative humidity.

S2.3 Hydrological model input data

S2.3.1 Inflow and outflow discharge

Stream discharge is observed only for the two major inflows River Ammer and River Rott plus the River Kienbach (Table S7). The hydrological contribution, concerning quantity and temporal distribution, of River Fischbach, of the other inflows (all other smaller creeks summarized, see Fig. 7 in the main text), and of the groundwater is unknown. To be able to reproduce the lake level applying GLM, four different inflows are defined. The time series represent the discharge data from 1. River Ammer, 2. River Fischbach, 3. groundwater inflow, and 4. the sum of River Rott, River Kienbach, and all other unknown inflows. Hereby, the real contribution of the respective inflow is approached by adjusting the inflow factors during the lake level calibration process.

Values of River Ammer time series are observed at Weilheim station (Fig. 7, main paper). The temporal pattern of Fischbach discharge is highly controlled by the outflow of Lake Pilsensee (Büche, 2018). The discharge of Fischbach is estimated by a simple rainfall-runoff relationship. The hydrograph (Fig. S~~Fig. S~~10) is designed considering the retention of the lake showing a slow reaction of lake outflows on rainfall events (long smoothed decline of discharge) and the subsequent inflow to the water body (indicated by the quick rise of the hydrograph in the first days after the rainfall). With a runoff coefficient of 0.4 the estimated discharge for the simulation period averages to 0.67 m^3s^{-1}. This mean value corresponds to the only hydrological value for Lake Pilsensee existing in the literature of 0.4 m^3s^{-1} for the annual mean of the main inflow (Grimminger, 1982).

Subsurface inflow to Lake Ammersee is estimated from groundwater level observation at Wielenbach (Fig. 7, main paper) calculated by a stage-discharge relation (Fig. S11~~Fig. S11~~). The inflow is set to insert the lake at a depth of 79.15 m above the lake bottom, which is about 4 m below the surface (Bueche and Vetter, 2014) dependent on the lake level.

The outflow of Lake Ammersee is observed at gauge station Stegen (Fig. 7, main paper) in a temporal resolution of 15 min. The discharge data are averaged and taken as outflow time series input data. After Kleinmann (1995) no subsurface outflows exist.

Table S7: Characteristics of sub-catchments of Lake Ammersee. The data are representative for the stream inlet to the lake

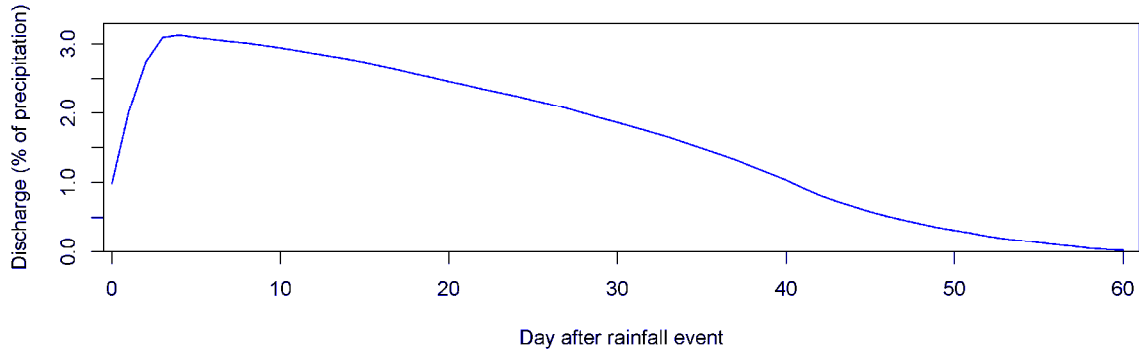| (Sub)-Catchment	Gauge station	Catchment size (km²)	Percentage of total area (%)
Ammersee	Stegen	994.6	100.0
Other inflows	-	122.0	12.3
Fischbach	-	56.2	5.6
Kienbach	Herrsching	12.4	1.2
Rott	Raisting	82.5	8.3
Ammer	Weilheim	721.5	72.5

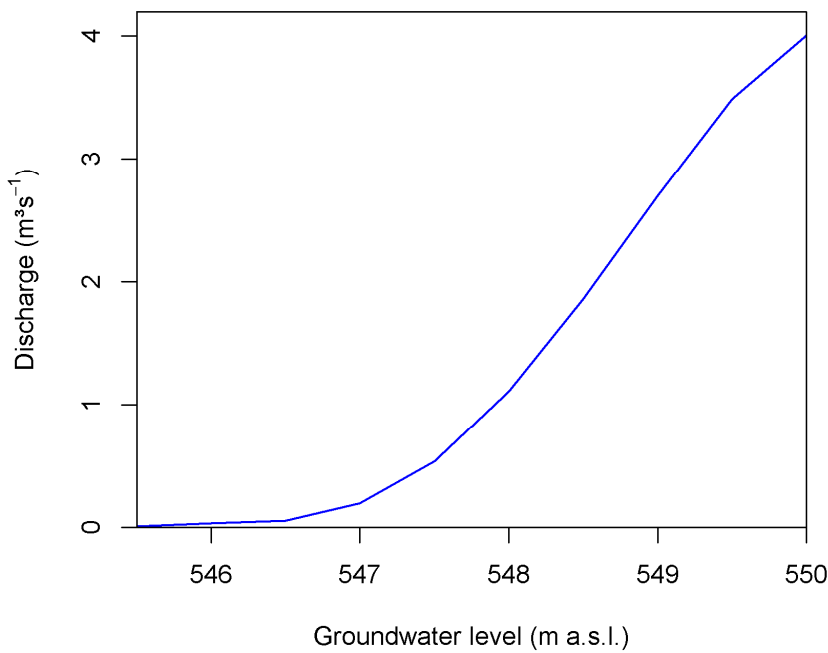**Fig. S10: Hydrograph of River Fischbach for a rainfall event.**

Fig. S11: Stage-discharge relation for groundwater inflow to Lake Ammersee.

The discharge of Rott, Kienbach and all other unknown smaller creeks are defined as one discharge time series to the simulation. Missing values for Rott and Kienbach (maximum gap length = 9 days) are estimated by expert knowledge taking rainfall events into account. The discharge of the smaller inflows is calculated from Kienbach gauge data multiplying the values by the factor of 8.28 representing the relationship of the sub-catchment area sizes. This is feasible as Kienbach and the smaller inflows have similar characteristics in relief and runoff generation.

S2.3.2 Inflow water temperature

Observations for inflow water temperatures are only available for River Ammer surveyed in hourly resolution (Gauge station Weilheim, Fig. 7, main paper) and values for water temperature are only specified for this surface inflow. However, these data can be seen as representative for the sum of all surface inflows. Water temperatures of groundwater can be estimated to be roughly equivalent to the annual air temperature (Boehrer and Schultze,

12

2008) and a constant value of 8.65 °C derived from long-term average air temperature (Bueche and Vetter, 2014) is applied for the subsurface inflow input data.

S2.4 Lake filed data

The water temperatures of the lake are observed automatically by a lake buoy operated by the Bavarian Environment Agency. Data are surveyed in the depths (all in given in m) 0.5 (representing the surface), 1.0, 2.0, 4.0, 6.0, 8.0, 10.0, 12.0, 14.0, 16.0, 18.0, 20.0, 25.0, 40.0, 60.0, and 78.0 in a temporal resolution of 15 min, but already provided by the operator as daily averages. The available data is displayed in Fig. 2 (main paper, black dots) and these values are used as field data. Existing temperature values in May 2016 are evaluated as unrealistic high and excluded from the data set. Lake level data are observed at Stegen gauge station (Fig. 7, main paper) in a temporal resolution of 15 min, but also as daily means are provided. The data unit is elevation a.s.l.. To obtain lake level heights the values are subtracted by the elevation of the lake bottom (449.78 m a.s.l.).

References

An, N., Hemmati, S., and Cui, Y.-J.: Assessment of the methods for determining net radiation at different time-scales of meteorological variables, Journal of Rock Mechanics and Geotechnical Engineering, 9, 239-246, https://doi.org/10.1016/j.jrmge.2016.10.004, 2017.

Bay. LfU, Bayerisches Landesamt für Umwelt: Gewässerkundlicher Dienst Bayern, https://www.gkd.bayern.de/, 2018

Boehrer, B., and Schultze, M.: Stratification of lakes, Reviews of Geophysics, 46, RG2005, 10.1029/2006rg000210, 2008.

Büche, T.: Ableitung des Wasserhaushaltes des Pilsensees aus Niederschlagsdaten - Erste Abschätzungen zum Ausflussgang des Pilsensees., Beiträge zum 49. Jahrestreffen des Arbeitskreises Hydrologie vom 23.-25. November 2017 in Göttingen, *GEOGRAPHICA AUGUSTANA*2018

Bueche, T., and Vetter, M.: Influence of groundwater inflow on water temperature simulations of Lake Ammersee using a one-dimensional hydrodynamic lake model, Erdkunde, 68, 19-31, 10.3112/erdkunde.2014.01.03 2014.

Chessa, P., Cesari, D., and Delitala, A.: Mesoscale precipitation and temperature regimes in Sardinia (Italy) and their related synoptic circulation, Theoretical and applied climatology, 63, 195-221, 1999.

Giadrossich, F., Niedda, M., Cohen, D., and Pirastru, M.: Evaporation in a Mediterranean environment by energy budget and Penman methods, Lake Baratz, Sardinia, Italy, Hydrology and Earth System Sciences, 19, 2451-2468, 10.5194/hess-19-2451-2015, 2015.

Grimminger, H.: Verzeichnis der Seen in Bayern, edited by: Wasserwirtschaft, B. L. f., München, 1982.

Hipsey, M. R., Bruce, L. C., and Hamilton, D. P.: GLM - General Lake Model: Model overview and user information. AED Report #26, The University of Western Australia Technical Manual, 22, 2014.

Hipsey, M. R., Bruce, L. C., Boon, C., Busch, B., Carey, C. C., Hamilton, D. P., Hanson, P. C., Read, J. S., de Sousa, E., Weber, M., and Winslow, L. A.: A General Lake Model (GLM 2.4) for linking with high-frequency sensor data from the Global Lake Ecological Observatory Network (GLEON), Geoscientific Model Development Discussions, 1-60, 10.5194/gmd-2017-257, 2017.

Idso, S. B.: A set of equations for full spectrum and 8- to 14-μm and 10.5- to 12.5-μm thermal radiation from cloudless skies, Water Resources Research, 17, 295-304, doi:10.1029/WR017i002p00295, 1981.

Kleinmann, A.: Seespiegelschwankungen am Ammersee. Ein Beitrag zur spät-und postglazialen Klimageschichte Bayerns, Geologica Bavarica, 99, 253-367, 1995.

Lavagnini, A., Martorelli, S., and Coretti, C.: Monthly maps of daily global incident solar radiation in Italy, Il Nuovo Cimento C, 13, 769-782, 10.1007/bf02507969, 1990.

Niedda, M., Pirastru, M., Castellini, M., and Giadrossich, F.: Simulating the hydrological response of a closed catchment-lake system to recent climate and land-use changes in semi-arid Mediterranean environment, Journal of Hydrology, 517, 732-745, http://dx.doi.org/10.1016/j.jhydrol.2014.06.008, 2014.

Pirastru, M., and Niedda, M.: Evaluation of the soil water balance in an alluvial flood plain with a shallow groundwater table, Hydrological Sciences Journal, 58, 898-911, 10.1080/02626667.2013.783216, 2013.

Springer, J., Ludwig, R., and Kienzle, S. W.: Impacts of Forest Fires and Climate Variability on the Hydrology of an Alpine Medium Sized Catchment in the Canadian Rocky Mountains, Hydrology, 2, 23-47, 10.3390/hydrology2010023, 2015.